Title
SOME EXPERIMENTAL SHIELDING STUDIES AT THE 6.2-BeV BERKELEY BEVATRON

Author
Smith, Alan R.

Publication Date
1965-11-10

UCRL-16323

University of California

Ernest O. Lawrence Radiation Laboratory

SOME EXPERIMENTAL SHIELDING STUDIES
AT THE 6.2-BeV BERKELEY BEVATRON

Berkeley, California

DISCLAIMER

Submitted to the Proceedings of the
First Symposium on Accelerator Radiation
Dosimetry and Experience

UCRL-16323

UNIVERSITY OF CALIFORNIA

Lawrence Radiation Laboratory
Berkeley, California

AEC Contract No. W-7405-eng-48

SOME EXPERIMENTAL SHIELDING STUDIES AT THE 6.2-BeV BERKELEY BEVATRON

Alan R. Smith

November 10, 1965

spectra over the energy range 2.0 to 30 MeV for several positions within the shield array. These spectra were obtained from the same activation detector data, but processed by methods developed recently at our Laboratory and described in another paper at this symposium.

Our third experiment relates to the energy spectrum of neutrons emerging from the accelerator shield in the vicinity of a thick target, one of the plunging magnets used to extract the circulating proton beam. We use the mixed system of threshold detectors here, including moderated foil or BF_3 counter, aluminum disk, carbon (in the form of plastic scintillator), and bismuth fission counter. Our analytical method is to combine detector calibrations, reaction-cross-section data, and trial neutron spectra to calculate a detector response that matches the observed response. A simple computer program performs the arithmetic work, and easily permits variation of all input parameters. We show how some reasonable variations in these input parameters affect calculated detector response, and then describe the neutron spectrum that best fits our observed detector response. At sites where the moderated BF_3 counter reports a fast-neutron-flux intensity of about 30 n/cm^2-sec, such measurements are performed in a 1-hour simultaneous exposure of all detectors, followed by an approximately equal counting period. Longer exposure time for aluminum disks and the bismuth fission counter permit extension of this technique to flux intensities as low as 1 n/cm^2-sec.

The foregoing is in the nature of a progress report. Several facets of our technique are in need of improvement, and there exists a serious lack of some basic data upon which the accuracy of results depend: for example, neutron-reaction cross-section data. We wish to illuminate clearly these areas of incomplete knowledge, and hope that recognition of their existence will stimulate interest toward closing the gaps.

I. INTRODUCTION

As particle accelerators become capable of producing beams of higher energy and greatly intensity, the role of radiation shielding becomes even more important. We must provide adequate protection for those who work around or live near such accelerators, and so the proper amount of shielding must be interposed between these people and the sources of radiation. The cost of this shielding, in terms of money and time, is now a major factor in both the design of the accelerator itself and the experiments performed at this facility. The sheer bulk of shielding employed at multi-BeV accelerators is so great that it is quite important to be able to specify closely the amount of shielding required for a particular situation. At these large machines it is not reasonable, for example, to include a safety factor of 10 in shield design simply to compensate for possible errors in design concepts. A tenfold attenuation for high-energy neutrons and protons may require a 4-foot thickness of ordinary concrete. It is evident, then, that we must have a clear understanding of the important parameters related to shield performance, in order that actual performance will closely match design calculations.

It is toward such an understanding that we describe some recent experience gained at the Berkeley Bevatron. We report three kinds of experiments, all related to shield performance and the characteristics of the radiation against which shielding must be provided. We are concerned mainly with measurement of the spectra and intensities of particle fluxes, because it is these quantities that we feel are most meaningful for describing shielding studies at high-energy accelerators. As we have seen in a previous session of this meeting, flux intensity and spectral information can be converted into biological hazard quantities when that is required; the converse is not true.

We first describe an experimental evaluation of the improvement in shield effectiveness accomplished by installation of a complete shield structure around the Bevatron. We compare the measured value with the value predicted by shield design calculations. We then discuss some attenuation measurements and neutron spectral information obtained from a large concrete shield array when this array was bombarded by the 6.2-BeV external proton beam. In the last study, we report some neutron spectral information obtained at stations that were outside the shield but were in the vicinity of a thick target located inside the accelerator. In summary, we then show how these sets of results are complementary parts of a general picture that is consistent with the attenuation and spectral characteristics observed for the nucleon component of the cosmic radiation.

I draw heavily on the work and publications of other members of the Berkeley LRL Health Physics Department, and hope that credits given them in a later section convey the importance of their contributions to the progress reported here. To a considerable extent, this paper is the summary of a group effort for which I am the spokesman today.

I do not attempt to summarize the results of similar studies performed at other laboratories, nor do I make detailed comparisons between such studies and our results. It is my purpose simply to describe our work. Comparison with other studies, critical comments, and suggestions for further work, can then be made in full light of results, but unencumbered by our valued judgements; hopefully, such topics will receive attention in the discussion period that follows this presentation.

II. EVALUATION OF BEVATRON-SHIELD IMPROVEMENT

The Bevatron ceased operation in June 1962 to permit extensive modification and improvement. Among the improvements was installation of a complete shield around and over the machine. Prior to this installation, the Bevatron shield consisted principally of a vertical wall of concrete encircling the accelerator and standing somewhat taller than the magnet structure. Wall thickness varied from 5 to 10 feet, with greatest thickness in the vicinity of target locations. The ring shield was augmented at the four straight sections by roof shields added as the need became apparent. We show a view of this shield arrangement in Fig. 1.

We performed an extensive series of radiation surveys around the Bevatron during March through June, 1962. These measurements were designed to provide one set of data for evaluation of the shielding improvement brought about by installation of the complete shield; a second set of data would be acquired after resumption of accelerator operation. We planned to do these measurements early in 1963, Bevatron operation permitting.

The improved shielding provides a complete roof over the accelerator, as well as greater thickness along most of the ring wall. The roof is so designed that any particles emerging from straight sections (the weak spots of the accelerator structure, in the shielding sense) must penetrate a minimum of 7 feet of concrete to reach the outside of the shield; the walls are now 10 feet thick. Details of shield design were described by Moyer.[1] We show a view of the new shield structure in its relationship to the Bevatron in Fig. 2.

The most important kind of data gathered in the 1962 surveys came from activation-type neutron detectors, that could integrate over periods of many hours. Gold foils in cadmium-clad moderators measured the total fast-neutron-flux intensity; aluminum disks, 4-in. in diam by 1-in. thick, responded only to that portion of the fast neutron flux with energy greater than 6 MeV. Calculations for the new shield predicted we could easily repeat these measurements when Bevatron intensity reached the order of 1×10^{13} ppp (protons per pulse).

When the Bevatron resumed operation in early 1963, our desired high-beam intensity was not achieved during the relatively short time that suitable beam-target conditions prevailed. The external proton beam facility was brought rapidly into operation, and since that time the accelerator has produced an external beam almost constantly. The shield comparison cannot be made while the external-beam plunging magnets are in operation; when operated, these magnets are thick targets--strong sources of radiation. This radiation contributed significantly to the radiation pattern observed outside the shield, and so would make shield comparison data quite difficult to interpret. We decided to await the proper Bevatron conditions, meanwhile concentrating on the regular radiation surveys and working to improve our detectors and counting techniques.

A recent emulsion exposure provided a favorable opportunity to attempt the necessary second set of measurements. For the emulsion exposure an internal target located at 22° in magnet quadrant 3 was used--virtually the same target position as was used for Survey 1 of the 1962 series.[2] Although beam intensity for the emulsion exposure was only about 2.3×10^{12} ppp, the improvements in our techniques noted above made it possible to obtain good results at this reduced intensity. (The reason for success is not that shield performance falls below expectation.)

For both surveys, we located detectors along the crane walkway in the main building. The relationship of this walkway to the shield and the enclosed accelerator is shown to scale on Fig. 3. Twenty four detector sets per survey were used, each consisting of a moderated gold foil and an aluminum disk. A set was placed at the center of each bay, thus completely encircling the accelerator. Gold-foil detectors were identical for both series of measurements. In 1962, aluminum disks were 4-inches in diameter and 1-inch thick; in 1965, aluminum disks were 8-inches in diameter and 1-inch thick, and were counted with a large NaI(Tl) crystal. The size increases were required for successful measurement of the decreased flux intensities. Additional sets of detectors were placed on the shield roof directly above the circulating beam orbit; information obtained from these detectors was related mainly to other studies and will not be discussed here.

Gold-foil activity is normally measured with a gas-flow proportional counter, one foil at a time. Because of the shortness of the 1965 exposure and the small relative magnitude of neutron fluxes, the activity induced in most foils at craneway stations was too small for determination with the flow counter if reasonable counting times were employed: 200 to 500 minutes, for example. These foils could be analyzed successfully with our NaI(Tl) scintillation crystal gamma-ray spectrometer, by the simple expedient of counting foils in groups. Ten to twenty foils could have been counted together but we used groups of four or five in order to preserve some detail in the radiation profile.

A. Exposure Information

Irradiation time for the 1962 survey was 112 hours, and for the 1965 survey was 13.5 hours. Accelerator operation remained constant throughout both exposure intervals. A detailed record of the integrated total of the accelerated proton-beam magnitude was kept in each case. From these records, we determined the average beam intensity that belonged with each exposure; we also made accurate corrections for the degree of equilibrium activity attained for the two half-lives of importance. All detectors were placed at, and removed from, irradiation sites while the accelerator was OFF; this precaution could have been of some importance for the short 1965 exposure time.

Proton-beam intensities for the two studies, corrected as indicated above and adjusted to a machine repetition rate of 11 pulses per minute, are:

$$1962: \ 1.1 \times 10^{11} \text{ ppp}$$
$$1965: \ 2.32 \times 10^{12} \text{ ppp.}$$

The recent beam intensity is about 20 times that of the previous intensity.

B. Results

In the discussion that follows, we describe the 1965 measurements in considerable detail; we then present pertinent information regarding the 1962 measurements. The shield evaluation is based on comparison of these two measurement sets.

Detailed results are presented in graphical form, showing neutron-flux profiles in relation to the circular accelerator structure. Figure 4 shows the fast-neutron-flux profiles determined in 1965; the upper profile represents moderated gold-foil detector fluxes, and the lower profile represents aluminum-disk threshold-detector fluxes. These values are appropriate to a steady circulating-beam intensity of 2.32×10^{12} ppp at a rate of 11 pulses/minute, or an equivalent intensity of 4.25×10^{11} protons/sec; beam energy is 6 BeV.

Some detail in the total flux profile on the craneway has been lost because of the group counting of Au foils. However, little detail was expected, and so we have probably not lost much useful information. For example, compare moderated foil data and aluminum-disk data at Bays 6 through 9. These four Au foils were counted singly. Note that the foil-data profile is much smoother than the aluminum-data profile; we expect a similar relationship to exist elsewhere along the craneway. Numbers that appear beneath points along the foil profile denote grouping of foils for activity analysis. The main purpose of this measurement set required that results

from all 24 bays be summed; the loss of detail is of no consequence in this context.

Aluminum-disk data is reported in terms of n/cm^2-sec, but with a special meaning attached to the flux units. Values listed are the fluxes of 14-MeV neutrons (the energy used for detector calibration) that would have produced the observed detector activations. Although these values do not represent actual flux intensities for the spectral composition of the neutron field under investigation, they are useful for point-to-point comparisons in one profile, and for profile-to-profile comparisons when experimental or shielding conditions are changed.

The aluminum-disk craneway profile shows considerably more structure than the companion Au-foil profile. Each tangent tank, except the WTT, is a relatively strong neutron-emitting area compared to magnet quadrant areas. It is doubtful that the target (located in O-III at about Bay 2) can be seen through the combination of magnet-iron and concrete-roof shield. However, tangent tanks can be seen through the concrete roof shield; there is no magnet iron at these places.

Craneway disk activities were so small that all 24 detectors could not be counted before decay of the 15-hr Na^{24} activity had reduced some disk activities beyond reach. Fifteen disks were counted, and the other nine points along the profile were obtained by drawing "reasonable" lines across gaps.

C. Evaluation of Shield Improvement

Bevatron operating conditions for the 1965 data are considered to be nearly identical to the 1962 conditions, except for beam intensity and shield configuration. Beam-intensity differences are easily taken into account; thus we can evaluate the improvement in shielding, as recorded by these neutron detectors.

The 1962 craneway profiles are shown on Fig. 5, where the upper profile is moderated Au-foil data, and the lower profile is aluminum-disk data. These neutron fluxes are appropriate to a steady circulating beam intensity of 1.0×10^{11} p+/pulse at 11 ppm, or a rate of 1.83×10^{10} p+/sec.

We make the shield evaluation in the following manner. Flux values (measured or interpolated) for all 24 equally spaced survey stations are summed and average values computed. The 1965 values are normalized to the 1962 beam intensity. Ratios between 1962 and 1965 fluxes are then taken to be numerical factors of shield improvement. This information is summarized in Table 1.

Note that moderated foils indicate an improvement factor of about 430, whereas aluminum disks indicate a considerably smaller factor--about 90. This result is consistent with our understanding of the neutron field that exists around the Bevatron, as described briefly in the following.

In 1962 the magnet top was almost completely open (unshielded), and acted as a strong source of low-energy neutrons (< 1 MeV); these neutrons could easily reach the craneway stations to be detected by moderated Au foils. In 1965 the top shield completely absorbs this component of the neutron field; the neutrons now seen outside the shield are only those that are produced by, or exist as, "high-energy" particles when they leave the accelerator structure. One consequence of this situation is our expectation that the 1965 spectrum would be richer in high-energy neutrons than was the 1962 spectrum. The greater relative response of the aluminum detector in 1965 confirms the expectation.

Measurement of "average neutron energy," performed with moderated BF_3 counter and polyethylene-lined counter, also agrees with the above picture. Typical 1962 values obtained on the main floor outside the shield were about 0.2 MeV; typical 1965 values for the same stations are 1.0 to 1.5 MeV. In 1962, the average neutron energy increased as one moved away from the accelerator, until a value of about 1 MeV was observed at a distance of 700 to 900 feet. No further increase was noted for this quantity at greater distances. We do not now observe any significant change in mean energy related to distance from the Bevatron. We attribute such behavior to the effect of the top shield–that is, the presence of the easily absorbed low-energy component in 1962, and the absence of this component in 1965.

We can phrase the shield-improvement results in another way, using the neutron-field model just described. The value obtained from moderated Au foils, when adjusted for the RBE changes that belong with changes in neutron energy, should be appropriate for locations close to the accelerator: the experimental and work areas in and around the Bevatron building. The aluminum-disk values should be appropriate to more remote locations, such as other buildings at the Laboratory and the perimeter of the project area. Henry Dakin,[3] of our group, recently completed another set of shield-evaluation measurements, using the same "before" and "after" Bevatron operating conditions. In his survey, a moderated BF_3 counter measured total fast-neutron flux, and a shield-improvement factor of about 80 was observed for a station 1000 feet from the Bevatron. This result is in good agreement with aluminum-disk data.

In 1962 the accelerator was only partially shielded, but in 1965 it is completely surrounded by a thick concrete shield. We do not now expect changes in the shield to alter the shape of the neutron spectrum significantly. Consequently, we should be able to measure future changes in shield effectiveness with either type of detector employed here, and expect to obtain closely similar results from careful measurements. Of the two types, greater care must be exercised when using moderated foils, because the foils are sensitive to low-energy neutrons. The population of such neutrons can be strongly enhanced by certain arrangements of shielding materials, and shield evaluations made under these conditions may appear to give puzzling results. The aluminum detector, with its >6-MeV threshold

energy, is relatively unaffected by such circumstances, and should provide more directly understandable results in terms of shielding against high-energy particles. Use of both types simultaneously is preferable to use of either one alone. Such practice provides considerably more than a simple doubling of acquired information, because one also learns something about gross changes in neutron spectral distribution.

One important aspect of these studies is to provide a meaningful basis for comparison between measured and calculated values. Thus we would like to compare our measured fluxes with those predicted by Moyer[1] from his calculation of Bevatron shielding. Our data are not directly applicable for such a purpose; and when such a comparison is attempted, our data requires considerable adjustment to match the calculation conditions. This adjustment procedure could introduce errors that might obscure the precise meaning of the comparison.

We can, however, make a general statement regarding these measurements and Moyer's calculations. His calculations predicted that emission in the upward direction of very high energy (above 150 MeV) neutrons would be reduced a factor of ≈ 100 as a consequence of shield improvement. Although we have not directly measured these neutrons, the aluminum threshold detectors measured a neutron flux that is reasonably expected to be proportional to his calculation flux. Insofar as this assumption is true, calculations and measurements are in good agreement: calculations predict a factor of about 100, and measurements indicate a factor of about 90. The question of precision then involves the extent of validity in assuming proportionality between the two fluxes; we are studying this problem. We will also undertake another series of measurements, designed to match more closely the calculation conditions, and hope to refine the comparison values through such efforts.

We feel the practical terms for evaluation of shield improvement have been met in the study presented here, and that future efforts in this direction will be to refine, rather than to revise, the results. We emphasize that measurements and calculations agree quite closely; furthermore, these calculations were based on concepts of the radiation field and shield behavior that are consistent with results reported in other sections of this paper.

III. SHIELD-ARRAY EXPERIMENT: ATTENUATION MEASUREMENTS AND NEUTRON ENERGY SPECTRA

A. Description of Experiment

The experiment concerns the shielding of high-energy particle accelerators. For this purpose, we used the 6-BeV external proton beam produced by the Bevatron. Figure 6 shows a plan view of the experimental setup. The primary proton beam entered from the right along a shielded channel, which narrowed to a 2- by 2-ft cross-section area about 8 ft ahead of the shield array. A thin plastic scintillator at the front of the narrow channel was viewed by closed-circuit television. The position and size of

the beam spot were continuously observed in this fashion; correct beam alignment was verified by reference to a grid scribed on the scintillator. The longest dimension of the beam spot was usually no greater than 2 in. as viewed by the scintillator-television system.

The shield array consisted of ordinary concrete in block form, and was 28 ft thick along the beam line, 22 ft wide, and 18 ft high. Slots provided access to the beam line at 4-ft intervals. Several special thin blocks at the front of the array allowed more detailed study in this region; access was from the top for these positions. Rows of blocks were separated by 3-in.-wide gaps to allow insertion of detectors. All portions of these gaps, except the 18-in.-high slots actually used for detector placement, were filled with gypsum wallboard to minimize air spaces along which neutrons could scatter or diffuse.

Figure 7, a photograph of the working face of the array, gives some idea of the actual setup and the manner in which it was used. A wooden trough loaded with detectors has just been inserted in one of the slots; all detectors were positioned for exposure in this fashion.

The principal detectors are the activation-threshold type. In such a detector, an integrated response that can be produced only by neutrons (or protons) whose energy is greater than some "threshold" value. When several elements are so used, each having a different threshold energy, we can obtain information related to behavior of different energy groups in the experimental constraints. Ultimately, one may be able to construct a neutron (or proton) spectrum from these data.

Figure 8 shows a set of detectors arranged in the wooden troughs, ready for exposure at beam-axis positions in the shield array. Among the elements employed are: aluminum, carbon, cobalt, copper, iodine, iron, magnesium, nickel, and titanium. These materials are in the form of 4-in.-diam disks, ranging in the thickness from 1/32 to 1 in. With one exception we observed the gamma-ray activity of radioisotopes produced during irradiations; this exception was carbon. Here we used carbon in the form of a plastic scintillator, and detected the positron decay directly inside the scintillator.[4] From all other materials, we obtained multichannel gamma-ray spectra with a sodium-iodide-crystal scintillation spectrometer. Spectra were studied during decay of the various isotopes until we could obtain quantitative results for each isotope of importance.

B. Attenuation Measurements

The shield structure existed for two months, and during most of that time it served as the external-beam backstop for a physics experiment. Much of the period was suitable for our purposes, and it was at such times that we developed a series of attenuation profiles within the array. Gold foils, aluminum disks, and carbon scintillators were so employed, to provide information about three neutron-energy groups. Detector activities were observed at every 4-ft depth, laterally from the beam axis to the

shield's edge at 1-ft intervals. From these data we constructed detailed radiation profiles for all positions inside the shield array, as viewed by these three detectors. Most exposures were made when the external-proton-beam intensity ranged from 10^{10} to 10^{11} protons per second; exposures varied in length from about one to several hundred minutes. Careful attention ensured that each exposure provided normalization data so that all results could be related within a single comprehensive framework.

C. Presentation Format

Essentially all the useful data presented here is in graphical form. In an effort to enhance the value of this graphical information, Figs. 9 through 13 are reproduced full size; that is, one can retrieve detailed numerical values by simply tracing our curves on standard 8-1/2 by 11 inches sheets of graph paper. Figures 9, 10, and 13 are drawn on semilogarithmic paper, with 7 cycles vertically and 10 divisions per inch horizontally, Keuffel and Esser type 359-96, or equivalent. Figures 11 and 12 are drawn on Cartesian-coordinate paper, with 10 divisions per centimeter both vertically and horizontally, Keuffel and Esser type 359-14G, or equivalent.

Figures 10 through 13 are sets of triplets, for which we adopt the following convention: gold data are presented as the "a," aluminum as the "b", and carbon as the "c" member. We emphasize characteristics of the radiation field as reported by the carbon scintillators, because this type of detector has the highest energy threshold in the group and should therefore provide the most meaningful information for shield design. Discussion of these figures is based on the carbon member in each set, and the other detectors merit discussion only when their response differs significantly from that of the carbon detector.

D. Results

Figure 9 shows attenuation profiles measured along the beam axis by the three detectors. Plotted points are actual data points, normalized to identical activity at the 8-ft position, for ease of comparison. The gold reaction, a thermal-neutron capture, is also a valid indicator of total fast-neutron flux as used here; the aluminum reaction has a neutron threshold energy of about 6.7 MeV; and the carbon reaction has a neutron threshold energy of about 20.4 MeV. Aluminum and carbon reactions can both be initiated by protons of somewhat higher energies. We see that the slopes of all three curves become similar at great shield depths, but are clearly not identical. We take the carbon curve to be most representative of the high-energy component within the shield. The 1/e attenuation length observed along the straight portion of this curve is 108 g/cm, with 2.4 g/cm^3 used as the density for ordinary concrete.

Figure 10(c) shows lateral profiles taken at each 4-ft depth by the carbon detectors. The shield edge is at about 11 ft on the abscissa. Profiles change smoothly from concave upwards near the shield front to convex upwards at great depths. From data taken at the greatest depth, it is evident that we are approaching the condition in which the profiles approximate plane wave fronts. Several simple transformations of this data have been performed; three of these are presented inFigs. 11 through 13.

Figure 11(c) shows carbon profiles of constant attenuation at lateral positions relative to the intensity along the beam axis normal to each position. Curves show fractional values of beam-axis intensity at off-axis positions. For example, at 16-ft depth, the intensity decreases a factor of 100 at 9-ft off-beam axis. Irregularities in Fig. 6(a) gold profiles are thought to be caused by local inhomogeneities in the thermal neutron-capture properties at such sites.

Figure 12(c) shows constant-intensity contours existing within the shield array. The values listed with contours are in terms of neutrons/cm^2-sec (or protons/cm^2-sec) for a 6.2-BeV proton beam of about 1.7×10^8 protons/sec incident on the shield array; the reaction cross section to produce carbon-11 is taken to be 30 mb.

Figure 13 is constructed from the contours presented in Fig. 12. Points plotted on Fig. 13 represent intersections of selected paths through the shield with contours of Fig. 12. The origin for this transformation is taken to be the point at which the beam strikes the front surface of the shield. We plot detector activity versus path length through the array, taking several different angles with respect to the beam line.

Figure 13(c) shows the resulting attenuation curves for the carbon detector. The uppermost curve, the 0-deg or beam-axis profile, is shown for reference. The four other profiles are, in order downwards, at 10, 20, 30, and 45 deg. The significant feature of these curves is that all slopes are essentially identical. That is, the mean attenuation length appears to be constant for all angles to 45 deg, at all depths beyond about 5 ft, when we measure distance from the point of beam incidence. A reasonable extrapolation of the data indicates that the same attenuation length is observed at an angle of 60 deg.

The aluminum curves of Fig. 13(b) show the same slope similarity for all angles investigated--to 60 deg. The gold curves of Fig. 13a show the same similarity for all angles through 30 deg, but exhibit increasing slope (more rapid attenuation) at greater angles. Data points for the high-angle profiles lie close to the shield edge, and loss of thermal neutrons by diffusion out of the slots may account for this effect.

Our methods of data acquisition and normalization are described in some detail, because their nature has considerable bearing on the appearance of attenuation profiles. We included at least one detector at a standard, or monitor, position for each exposure that contributed data to the

profiles. This position was always on the beam axis, and always at least 8 ft from the shield front; most normalization detectors were located at a 12-ft depth. The site was selected because it was deep in the stack, and so should be relatively unaffected by beam steering variations, variations that might produce significant changes in flux intensities at beam-axis positions close to the shield front.

A typical run provided data for a complete lateral profile at one depth for one detector type, along with a monitor value. Profiles for each detector could then be incorporated into a single pattern, encompassing the entire shield array. Several exposures were made at beam-axis positions only, to determine as much as possible of this profile at one time. For gold and aluminum we were able to obtain data from single exposures that extended from 4-through 24-ft depths. The carbon beam-axis profile was obtained from several runs, in which at least one overlapping point provided connection with the other runs. We also made special simultaneous exposures of carbon and aluminum at the 12-ft position so that we could relate both profiles to a common beam intensity incident on the shield array.

With this description of our methods in mind, it is reasonable to expect that all points in each lateral profile will be self-consistent, and should be related to each other just as indicated by counting statistics. However, this is not necessarily true for the relationship among profiles taken at different depths. As data analysis proceeded, we began to notice that results from points close to the shield front were not always brought into as good agreement as one would like via the 12-ft normalization point; this is particularly true at 4-ft depth. For example, the aluminum profile at beam-axis positions was measured twice through the entire array in single exposures. All points at 12 ft and beyond are in good agreement; however, the 4-ft points do not match very well, and the 8-ft points are somewhat mismatched. The 4-ft mismatch is on the order of 30%--perhaps not a large difference considering the nature of the experiment, but still a disappointing situation.

The most reasonable explanation of these differences is lack of reproducibility in beam positioning from run to run. Since we did not control accelerator operation during attenuation profile runs, not much could have been done to improve the situation. Our periods of beam control were only for spectral measurement runs, and there was not time to do extra things during such intervals. We conclude that our profile pattern for the whole shield array is not so precisely determined as we first thought. In particular, the relationship of the 4-ft profile to the others is in some question. We think the 4-ft aluminum profile is somewhat lower than it should be. The 8-ft profiles seem nearly correct; also, all profiles at 12 ft and beyond appear to be correctly related. We believe the carbon profiles to be most precisely related through the entire array.

As our main interest concerns results obtained at depths beyond 8-to-12 ft, this purpose has been satisfactorily fulfilled. However, we would

like to be able to place greater confidence in front-position results, especially in view of some problems presently under discussion concerning the relative abundance of high- and low-energy particles behind thin shields.

We were able to obtain some attenuation-profile data during the occasional periods when the Bevatron operated at reduced beam energy. We acquired complete beam-axis profiles for the aluminum detector at proton energies of 4.2 and 2.2 BeV. These profiles appear as Fig. 14, where the three curves are arbitrarily adjusted to coincide near the 8-ft position, to aid in comparison of their slopes. Note that the mean attenuation length, determined by the straight portions of profiles, decreases from 114 g/cm^2 at 6.2 BeV, to 108 g/cm^2 at 4.2 BeV, and finally to 99 g/cm^2 at 2.2 BeV. These values are related to production of Na^{24} in aluminum by whatever reactions occurred to produce this isotope. It is not clear how to interpret these changes of slope, or attenuation length. Although the variation in attenuation length is only about 15%, and therefore of minor practical significance, it is a real difference observed with our experimental conditions and does need an explanation. Another interesting point concerns relative count rates in aluminum detectors for different beam energies. When normalized to the same incident beam intensity, the count rate for 6.2 BeV is triple the count rate for 4.2 BeV, at the 12-ft position. Unfortunately, we were not able to make a similar kind of normalization for 2.2-BeV energy.

Carbon and aluminum data from these profiles have also been converted into terms appropriate to our mixed system of threshold detectors through a simple transformation of count rates according to the sensitivities of the different size detectors. These converted values are used to provide data for Fig. 15. The information shown here represents values of the ratio between carbon and aluminum count rates, for various positions within the shield array. The upper curve shows values of this ratio for beam axis positions. Note that the ratio decreases with increasing shield thickness. Although we do not include all the relevant data here, we also observe that the magnitude of the ratio decreases as we move laterally away from the beam axis, except at a 24-ft depth where no change occurs; furthermore, the ratio never increases along a lateral profile. For example, Fig. 15 also shows the 4-ft lateral profile, where the ratio value is about 29 on the axis, and about 11.5 at a position 5 ft off the axis.

Although we are not certain of the absolute values for these ratios in view of normalization problems mentioned earlier, we do feel the general trend of values to be significant. This trend can be simply and reasonably related to our concept of particle interactions that occur inside a shield structure. Of these two detectors, carbon exhibits nearly uniform sensitivity to all neutrons/protons with energies above the reaction threshold, whereas aluminum response is strongly peaked in the first half-decade of energy above its reaction threshold. We would then expect greater relative response from carbon when a spectrum is richer in high-energy particles. The incident flux of 6.2-BeV protons produces just such a situation within

our shield array. These protons will lose energy and disappear more quickly than the comparable-energy neutrons they generate. This is true because the protons are charged particles and lose energy by ionization as well as by nuclear interaction, whereas neutrons lose energy only by the latter mechanism. The protons enter as particles of high energy only, but the produced neutrons are of all energies. The situation is then one in which protons (high energy) are attenuated more rapidly than neutrons (all energies), and so carbon response decreases relative to aluminum response as we move deeper into the shield. These high-energy protons proceed through the shield in a narrow forward-directed cone, and will not be observed at wide angles with respect to beam direction; thus we explain the relative decrease in carbon response at off-axis positions.

E. Discussion of Attenuation Measurements

We are aware that a number of points are raised by our results. We recognize that our experimental technique fell short of expectation, and cite as evidence the difficulty in normalizing data from different runs at the front positions. However, if we take only that portion of profiles for shield depths beyond 12 ft, we are confronted by several inadequately understood phenomena.

The first of these is the variation of slope (or attenuation length) with observed reaction. The slopes steepen as the threshold energy for the observed reaction increases. Thus, a thermal detector produces the profile of shallowest slope (120 g/cm^2 attenuation length), the aluminum detector shows an intermediate slope (114 g/cm^2 attenuation length), and the carbon detector shows the steepest slope (108 g/cm^2 attenuation length). These differences are small, but they are real and are rather easily observed when such a thick shield serves as the experimental facility. Other low-threshold reactions, such as Fe$\rightarrow$Mn^{54} (about 2-MeV threshold), show profiles with slopes intermediate between gold and aluminum. High-threshold reactions—such as Mg$\rightarrow$Na^{22}, Al$\rightarrow$Na^{22}, Ti$\rightarrow$Sc^{44}, and Cu$\rightarrow$Co^{58}—show profiles most similar to the carbon profile (the reaction C$^{12}\rightarrow$C^{11}). The single exception is C$^{12}\rightarrow$Be^{7}, which is most like the Al$\rightarrow$Na^{24} profile.

The second point concerns the observation that beam-axis profiles approach straight lines only at greatest shield depths, say beyond 12-16 ft. This is somewhat surprising, and suggests that quite a large thickness of concrete may be necessary to establish the equilibrium radiation field. In fact it is possible that such an equilibrium radiation field does not really exist, if one looks closely enough. Here again, this result may not have great practical significance, but is relevant to a thorough understanding of shield behavior. Furthermore, the curvature of profiles is in a sense that shows greater slope at greater depth. If we integrate the intensities measured along each lateral profile, we can compute the total flux at each depth. When these quantities are plotted against shield depth, the resultant profile shows even greater curvature than that of the beam-axis flux-intensity profile; the sense of the curvature is the same in both cases.

The third point concerns the relatively short attentuation lengths derived from our results. These values, determined from data taken at greatest shield depth, vary regularly with respect to threshold energy for the observed reaction. The sense of this relationship is such that shorter attenuation lengths are indicated from reactions with higher threshold energies. For 6.2-BeV proton-beam energy, a thermal neutron detector indicates a value of about 120 g/cm^2, whereas the reaction $C^{12} \rightarrow C^{11}$, threshold energy 20 MeV, indicates a value of about 108 g/cm^2.

The fourth point concerns the change in attenuation length observed when incident-proton-beam energy changes. We see that the attenuation length decreases as beam energy decreases. The aluminum detector indicates a change from about 114 g/cm^2 at 6.2 BeV to about 99 g/cm^2 at 2.2 BeV.

We now comment on our use of values for attenuation lengths, particularly in view of the apparent precision indicated. These values are based on a uniform concrete density of 2.4 g/cm^3, and simply represent a conversion of the 1/e attenuation distance for detector-count rates into values given in conventional units of g/cm^2. The attenuation lengths are obtained from straight lines drawn through at least four data points, representing a shield thickness of 12 ft minimum: the four points from 12 to 24 ft, for example. Although actual attenuation lengths are not known so precisely, we can distinguish various relative lengths. In the broadest sense, it is quite clear from data points that different attenuation lengths were observed, and our values then show these relative differences. The shield array stood unchanged throughout this experiment, and detectors were always positioned the same way at each location. Furthermore, in some cases several reactions were observed in a single detector element, and different attenuation lengths were then observed; here, we have eliminated the possibility that slightly different detector locations in successive runs could produce variation in results.

When attenuation factors of greater than 10^3 are observed, it is possible to observe such small changes without great difficulty. Our shield array provided just this sort of opportunity. Although the variations noted would not cause the designer to revise his shield calculations in any large degree, it would be of considerable interest to understand the reasons for the observed shield behavior. We conclude that, while we may understand the general behavior of shielding well enough to arrive at reasonable design calculations, we surely do not have a detailed comprehension of the interaction phenomena involved. It is desirable to acquire this detailed comprehension: the need for further experimental work is clear.

Our attenuation lengths are based on measurement of specific radioisotopes produced in selected target elements. In many cases, an observed reaction product can be produced from target nuclei in a variety of ways. In general, these isotopes can be produced by neutrons, protons, pi mesons,

or even gamma rays; however, we do not expect gamma-induced reactions to be very important. Our activations are seen to be the resultant of reactions with some complex fraction of the radiation field, and may not be simply related to any single component. The complexity of this relationship is expected to be greatest at beam-axis positions, where the highest-energy particles are most abundant. It seems reasonable that the nature of our results is directly related to this complexity, and that a satisfactory understanding of results can be obtained only when we have a clear understanding of the many nuclear-interaction paths available; more reaction-cross-section data is required here. A much-higher threshold-energy reaction is also very desirable in this context: the production of the α-emitter Tb^{149} from gold, for example. We are now working to improve the sensitivity for detecting this reaction, so that it may be useful here, as well as for neutron spectral determination.

The thermal-neutron-capture reaction is an important exception in the matter of reaction complexity. If we select an element with high thermal-neutron-capture cross section, then to a first approximation we do not care about isotopes produced by high-energy reactions, simply because the high-energy cross sections are so small compared to the thermal capture cross sections. It appears that such a slow neutron detector may be the best choice for measuring the attenuation of a neutron flux in a concrete shield. One note of caution is in order. We have mentioned that gold profile data exhibited irregularities that were significantly greater than could be due to counting statistics alone. We attribute such variations to local inhomogeneities in the neutron-capture capability of the concrete. We recommend the use of cadmium covers for gold foils as a means to eliminate this annoying problem; we would then observe activation in gold produced almost entirely by resonance capture at a few electron volts of neutron energy, an energy safely above the region in which most capture in concrete occurs.

F. Neutron Spectra

Several kinds of useful results were expected from this experiment. We were most interested in the neutron component of the radiation produced and propagated through the shield array, because this component usually determines the shielding requirements for high-energy accelerators. The use of activation-threshold detectors, within the formalism developed by John Ringle of our group,[5] held good promise for obtaining neutron-spectrum information. Briefly, this method is as follows: We determine the induced activations of exposed detectors by using gamma-ray spectrometric analysis. These activations then are used as input data for a digital-computer program, which calculates a neutron spectrum that would have produced the observed activations. The calculation uses detailed cross-section information for each activation reaction, over the energy range 1 to 30 MeV. The use of detailed cross-section data is an important departure from the usual procedure followed in threshold-detector methods.

Bevatron experimental conditions impose two new problems on the neutron-spectrum calculation method. The first of these is the presence of protons with energies capable of initiating some of the activation reactions. The second is the presence of both neutrons and protons with energies far beyond the range for which the method was initally intended. Direct application of Ringle's formalism to our Bevatron data was unsuccessful--that is, meaningful neutron spectra count not be obtained from threshold-detector activations.

During his stay with our group, A. D. Kohler[6] concentrated on these problems, and was able to incorporate reasonable solutions for them into a modified version of Ringle's program. He could then derive neutron spectra for some positions within the shield array over the energy interval 2 to 30 MeV. We draw freely from Kohler's paper (UCRL-11760) in the following discussion. The important changes and improvements introduced by Kohler are presented here without elaborate detail; such detail can be found in another paper of this symposium.[7]

1. Use of experimental reaction cross sections in place of those calculated from the continuum model of the nucleus;

2. Calculation of the amount of activation in threshold detectors caused by neutrons with energies above 30 MeV.

3. Solution for the spectrum from the set of integral equations by a least-squares technique.

The use of experimentally determined reaction cross sections is largely self-explanatory. We must emphasize that somewhat arbitrary choices were often necessary in cases of conflicting data, that data were very sparse and sometimes almost completely lacking, and that a certain amount of artistic selection entered into the values we now employ. Reaction-cross-section information is not nearly adequate for the potential of our method, particularly for the energy range above about 14 MeV; cross-section information is almost nonexistent for neutron-induced reactions above 30 MeV.

Calculation of the activations caused by particles with energies greater than 30 MeV is a very important item for us, simply because a significant fraction of detector activation may be due to these particles in shield-array sites. Failure to make this correction will cause distortion in the calculated spectrum. Our correction scheme involves the use of Be^7-production in carbon (polyethylene) as the experimentally determined high-energy activation quantity. We assume a reasonable shape for the high-energy portion of the neutron spectrum, and also estimate the threshold-detector cross-section shapes in this high-energy region. Both estimates are then combined with the Be^7 data to give a value of the correction for activation at energies greater than 30 MeV. The need for high-energy-reaction cross-section data here is obvious!

In the solution for the spectrum, a least-squares technique is employed. We avoid problems associated with instabilities of matrix inversion that are caused by errors in experimental data, by abandoning the solution method requiring matrix inversion. Instead, we use a scheme that seeks the best fit, in a least-squares sense, between "trial" neutron spectra and measured activations. The trial spectrum that most closely matches experimental activation data is then taken to be the neutron spectrum. We require that trial fluxes must everywhere be positive, as a means for stabilizing the solution.

The least-squares method, as we now use it, cannot reproduce fine structure in a spectrum as clearly as does Ringle's matrix-inversion methods. However, for our Bevatron data, which contain significant experimental errors in addition to approximate corrections, the least-squares method does give answers that appear reasonable. We now turn to these results.

On Figs. 16 and 17 we show log-log plots of the step-function solutions for neutron spectra at four off-axis positions; data for these graphs are also presented in numerical form, as Table 2. Straight lines drawn through each spectral set are seen to represent reasonable fits to the data, with a possible exception at the 8'-4' position. Numerical values for slopes of the lines are indicated, and we conclude that the neutron spectral shape depicted by these results is consistent with a $1/E$ number-versus-energy relationship over the energy range 2 to 30 MeV. Such a spectral shape is expected from our general concept of neutron interactions in concrete shielding.

For spectrum calculations at these four locations we used the following five reactions:

$$Ni^{58}(n, p)Co^{58}$$
$$Fe^{56}(n, p)Mn^{56}$$
$$Al^{27}(n, \alpha)Na^{24}$$
$$Mg^{24}(n, p)Na^{24}$$
$$Co^{59}(n, 2n)Co^{58} .$$

At the 4'-1' location we added a sixth reaction:

$$I^{127}(n, 2n)I^{126} .$$

Values we use for these reaction cross sections are described in Kohler's paper[6] and in an earlier presentation at this symposium.[7]

All neutron spectra shown in Figs. 16 and 17 are from locations within the shield array; however, all locations are off the beam axis. The correction for high-energy activation is largest along the beam axis, and

it is significant that beam-axis locations do not give meaningful spectral information at this time. We believe the reason lies in our inability to make the proper corrections for high-energy activation; large errors in large corrections make the method unworkable. If high-energy reaction cross-section data were available, we might be able to retrieve the situation to obtain beam-axis spectra, in addition to other results now in hand.

Much of the text and many of the figures which describe the attenuation measurements appeared originally as Ref. 8. For this section of the present report, we have added some attenuation results, along with a more detailed interpretation of our experimental observations. All the neutron spectral information is new. We are still at work on analysis of data from the experiment, and plan to issue a revision of Ref. 8 to include all useful results computed since the original publication date, September 1964.

We mentioned that our attenuation profiles are not as precisely related as we had hoped. We are also somewhat dissatisfied with results of the gamma-ray spectroscopy that served as input data for neutron spectrum computation. A number of gamma-ray-analysis problems would be greatly reduced, or perhaps eliminated, if a lithium-drifted germanium crystal were used as the spectrometer detector. Nothing can be done about these circumstances, short of performing the experiment again. There is considerable interest in such a project, especially in view of shield-design problems raised by study of construction of higher energy accelerators. If we do repeat the experiment, it will be as part of a larger effort, an effort that includes study of different shield materials as well as an investigation of shield behavior at larger angles with respect to the "target." Our present experience should serve as a valuable aid to successful execution of this larger experimental program.

IV. NEUTRON SPECTRA OUTSIDE THE ACCELERATOR SHIELD

The next series of measurements was made as part of an effort to clarify our understanding of the fast-neutron-energy spectrum that exists outside an accelerator shield. Past experience around the Berkeley accelerators has always supported the conclusion that this spectrum had a shape quite similar to the cosmic-ray neutron-energy spectrum, as reported by Hess, Patterson, and Wallace.[9, 10, 11] The evidence is in part that of experimental measurement of the spectrum itself; it is also based on evaluation of performance of shielding that has been designed to provide a particular attenuation factor if such a neutron spectrum did, in fact, exist within the shield structure. We cite evaluation of the improved shield at the Bevatron, described earlier in this paper, as an example; shield design is reported by Moyer.[1]

Some recent measurements from CERN[12] BNL[13], and HASL[14] suggest that with certain shielding conditions at multi-BeV accelerators, the spectrum may be much richer in high-energy neutrons than we would expect.

Although it is not clear how these particular shield conditions can be precisely described, it does appear that a relatively thin shield and a nearby target are required. These results are puzzling at present, and have acted as one stimulus for the measurements now described. Great interest in design of higher energy accelerators has been another strong incentive; and finally, our own interest in such matters has naturally brought about all the preparations necessary for actual performance of the study.

We employ the mixed system of threshold detectors here; this system includes moderated BF_3 counter or foil, aluminum disk, carbon scintillator[4], and the bismuth fission counter.[9] We have either two prompt counters and two activation elements, or one prompt counter (when a moderated foil is used) and three activation elements. If there is any possibility of count loss in the BF counter due to high instantaneous flux intensity, we substitute a foil (either indium or gold, depending upon the exposure length). We obtain spectral information for the neutron-energy range extending from about 0.02 MeV to 6.2 BeV, the full energy of accelerator-produced primary beam particles.

Detailed spectral shape can be obtained only when detectors have threshold energies spaced throughout the energy region of interest. Our highest threshold, about 50 MeV for the bismuth fission counter, is far below the primary particle energy, so this system can delineate only the broad character of a neutron spectrum. However, knowledge of reaction cross sections (or detector response) up to the primary energy allows the construction of rather narrow limits on the possible (and reasonable) actual spectral shape.

The relationships that exist among detector response (or reaction cross section), detector count rate, and neutron spectral shape have been explored with the aid of a digital-computer program. The reader is referred to an earlier paper of this symposium for relevant details.[7] We note that the spectral-analysis method is relatively insensitive to small errors in cross sections or response functions. The solution for a neutron spectrum is basically stable in a mathematical sense; furthermore, it is achieved through a simple and straightforward calculation procedure. In this procedure, we assume a trial neutron spectrum and compute detector count rates that belong with this spectrum. These count rates are compared with observed count rates; if differences exist, a new trial spectrum is constructed and the comparison repeated. Such a process may be continued until the desired agreement is obtained between computed and observed count rates; the trial spectrum at this juncture is considered to be the true neutron spectrum.

With these general remarks in mind, we now turn to some results obtained recently at the Bevatron. We use what are considered to be the most reasonable values for detector-response functions and compare count rates actually observed at the Bevatron with those computed from several other neutron spectra. These spectra include: a flat energy distribution; the 1/E energy distribution, the experimentally determined cosmic-ray

neutron-energy spectrum,[10, 11] and the neutron-energy distribution that provided a good fit for Bevatron experimental data. The latter three spectra are shown on Fig. 18.

This Bevatron spectrum is essentially a combination of the 1/E distribution at low energies and the cosmic-ray distribution modified for a 6.2-BeV energy endpoint; the two basic shapes are joined smoothly in the vicinity of 10 MeV. The spectrum shown here represents an average derived from five measurement sets, all obtained at the outer surface of the Bevatron's main shield. These stations were located in the vicinity of a thick internal target in the Bevatron STT, at angles that ranged from 90° to about 45° forward with respect to the beam-target line. Shield thickness varied from about 5-ft minimum to 14 ft maximum. For aluminum, carbon, and bismuth, the spread of values among individual sets is small relative to the averages shown here: all lie within ±15% of the averages. Moderated BF_3 counter response shows a wider range, with one value about 50% above, one about 50% below, and the other three within ±15% of the average value. Sensitivity to low-energy scattered neutrons is an important contributor to this behavior of the BF_3 counter.

The performance of our four detectors is shown graphically on Fig. 19, where we plot their responses to the different neutron spectra. All detector-response values are shown relative to that response observed in the Bevatron spectrum: the Bevatron response is taken to be unity for each detector. An additional normalization places all BF_3 values at unity, to emphasize contrasts among higher-energy detector response characteristics. The horizontal scale has no physical significance beyond that of arranging detectors according to reaction-energy thresholds. Note that aluminum, carbon, and bismuth responses to the cosmic ray spectrum are at least a factor of 2 below those for the Bevatron; also, that detector responses to the 1/E spectrum are at least a factor of 2 above those for the Bevatron. The important point is that we can tell differences among these spectra rather easily. Stated in another way, we observe that the method is sensitive to broad spectral differences, and is able to indicate clear choices without the requirement of extremely precise input data.

The method can be applied over a wide range of neutron-flux intensities. At locations outside accelerator shields, the problem is usually that the intensity may be too low (rather than too high) for successful measurement. It is in the context of low-intensity measurements that we have recently made greatest progress; to this area we now turn our attention.

A moderated foil or BF_3 counter can easily be made to provide the required sensitivity for low-intensity measurements. Our large bismuth fission counter registers about 1 count/sec when immersed in a uniform neutron-flux intensity of 57 n/cm^2-sec, at 200-MeV neutron energy; thus a flux intensity of 1 n/cm^2-sec at energy well above threshold will produce about 60 counts/hour. We require on the order of 200 counts per run from the bismuth fission counter in the interest of statistical value of results.

If we then assume a ratio of 10:1 between BF_3-indicated total fast-neutron flux and bismuth fission neutron flux, the lower limit on flux intensity for a 1-hour exposure is about 30 n/cm^2-sec, as measured by the BF_3 counter.

A 1-hour exposure is about three half-lives for the 20.4-min C^{11} activity observed in carbon scintillators, and is considered to be close to the maximum allowable exposure time for typical irradiation conditions. If carefully controlled constant-intensity conditions can be guaranteed, then there need be no limit on scintillator exposure time, but we usually are unable to specify such conditions and so impose this somewhat arbitrary time limit. We consider a 1-hour exposure to be compatible with scintillator activity half-life, if we can be certain that irradiation conditions remain reasonably constant during this interval. An interval during which accelerator-beam magnitude varied in a random fashion around one particular value would be an acceptable exposure condition; an interval during which the beam intensity erratically changed to a significantly different value would not be an acceptable irradiation condition.

The carbon scintillators for this work are 5 inches in diameter by 5 inches thick and weigh about 1700 grams. Our experimental calibration at 220-MeV neutron energy together with a calculation using a reaction-cross-section value of 22 mb indicated a count rate of 104 c/min from an immediate analysis following a long exposure at intensity 1 n/cm^2-sec.[4] If we use the BF_3 flux intensity of 30 n/cm^2-sec, and assume a carbon flux of 5 n/cm^2-sec, we would observe a count rate in excess of 400 c/min in the scintillator. This count rate is easily measured with good precision.

The aluminum disks are 8 in. in diam by 1 in. thick, and weigh 2.2 kg each; the NaI(Tl) crystal used for Na^{24} assay is 8 in. in diameter by 4 in. thick. The large size of this system is necessary because the 1-hour exposure is quite short compared to the 15-hr half life of Na^{24}. A 1-hour exposure produces only about 4.5% of the equilibrium amount of Na^{24} in a disk, so our potential sensitivity must be much greater than can be used in the present context.

At calibration neutron energy (14 MeV), irradiation of a disk to equilibrium in a constant flux of intensity 1 n/cm^2-sec will produce 70 c/min in our gamma-ray scintillation spectrometer system. We use the gamma-ray energy interval 1.29 to 2.90 MeV to define Na^{24} activity. This interval includes the two prominent gamma-ray peaks and the intervening continuum; it was selected to maximize the sensitivity for Na^{24} detection in our spectrometer system.

We again select the 30 n/cm^2-sec total fast-neutron-flux intensity, and assume a fifth of this flux to be the equivalent 14-MeV flux. We then observe about 16 counts/min due to Na^{24}-decay if a disk is counted soon after the 1-hour irradiation. At a BKG count rate of 95 c/min, we can determine this activation to ±7% in a 100-min count period.

From this brief description, it should be clear that the method is useful for flux intensities existing in areas that may be occupied a significant

fraction of the time. This comment pertains to the one-hour simultaneous exposure. When we can permit longer exposures for aluminum disks and the bismuth fission counter, much lower flux intensities can be studied successfully. Such matters are thoroughly documented in the earlier paper.

Our success in measurement of low flux intensities (small induced activations) is related directly to our ability to provide a counting environment in which the BKG rate is both very low and very constant.[15] In fact, without such a BKG environment these measurements would be impossible. We will omit detail here, and simply state that the BKG count rates in our spectrometer detectors are constant within the statistical significance of frequent long BKG runs; that is, within a small fraction of 1%. Use of a carefully maintained spectrometer system with this counting facility then permits us to accept as valid information net count rates that are small compared to the BKG rate. Spectrometer runs that produce low net count rate are always done carefully, but such runs are usual rather than unusual in our work.

For the C^{11} assay, we have been able to reduce BKG count rate in a plastic scintillator (5-in. in diameter by 5-in. thick) from the previous value of 700 to 800 counts/min to 125 counts/min. The improvement is due partly to use of the low BKG facility and partly to use of a 100-channel PHA for data acquisition. Use of this PHA permits very precise and reproducible selection of an upper boundary on the pulse amplitude accepted as valid C^{11}-decay events, while excluding all larger amplitude pulses that contain no C^{11} information. For the aluminum disk, low BKG in our large NaI(Tl) crystal is entirely due to the low BKG facility and the careful selection of low-activity components in the crystal-photomultiplier assembly; BKG in the Na^{24} interval is 95 counts/min. Both detectors produce a net count response from an equilibrium exposure to unit flux at calibration neutron energy that is nearly equal to the respective BKG rates. For carbon we have ~100 counts/min compared to 125 counts/min; for aluminum we have 70 counts/min compared to 95 counts/min. The net count rates are also relatively large numbers in both cases. This is an important consideration when half life is short, as in the case of carbon, or counting time is desired to be kept short, as in the case of aluminum.

V. SUMMARY

We have presented three kinds of shielding studies performed at the Bevatron. In each case we have studied the neutron component of the radiation field. In our experience at the Berkeley accelerators, it is this component that has proved to be most useful for shield design and evaluation; this component is also the most significant in terms of biological hazard.

Two of these studies–evaluation of improved Bevatron shielding and the spectral measurements near a thick target–are examples of work performed without requiring any special accelerator-operation conditions: that is, Bevatron operation proceeded entirely in accordance with the experimental physics program. The remaining study, the shield-array experiment, was in the nature of a full-scale experimental effort, requiring construction of the special array and control of the proton beam for a few hours of operating time.

We have described our experimental method for evaluation of improvement in Bevatron shielding, and have shown that the observed result, an improvement factor of about 90, is in good agreement with the calculated factor of about 100. This result gives strong support for confidence in general correctness of our shield-design methods--methods for which we assume existence of a neutron spectral distribution like that observe in the present studies. We have emphasized the value of high-sensitivity aluminum-activation-threshold detectors in this work.

The shield-array experiment has provided an enormous volume of data; much of this is as yet incompletely analyzed. We have obtained attenuation profiles for several of the threshold detectors; this information is immediately useful for shield design, particularly for high-energy beam back-stops. Neutron spectra measured at several off-axis positions in the array are consistent with spectral shapes obtained with our mixed system of threshold detectors. We have not been able to derive meaningful spectral results from detectors irradiated at positions along the proton beam axis, principally because we are unable to make the proper correction for high-energy particle contributions to observed detector activations. The paucity of high-energy neutron-cross-section data is the most serious obstacle to progress here.

Our measurements give somewhat shorter attenuation lengths than we expected. We also observe some variation of attenuation length that is dependent on the method of observation, even when we design this method to observe (mainly) the neutron component. The anomalies noted are not of a major significance in shield design; however, they are important to a detailed understanding of shield behavior. In this area, as well as in the domain of neutron spectroscopy with threshold detectors, progress would be more rapid and certain if the required cross-section data were available. The lack of cross-section data is particularly serious for neutron reactions at energies above 20 MeV. Without such data, threshold detectors fall considerably short of their potential value, either for attenuation measurements

or for neutron spectroscopy.

In our study of neutron spectra outside the shield but near a thick target, we have shown how the mixed system of threshold detectors indicates a particular spectral shape. The observed neutron spectra exhibit a 1/E shape in the energy region 0.02 to 10 MeV, and a somewhat steeper slope as the energy increases beyond 10 MeV. This slope is quite similar to that of the cosmic-ray-produced neutron spectrum, and appears reasonable in view of the nuclear interactions and energy-loss mechanisms that high-energy particles experience as they penetrate a massive concrete shield.[16, 17, 18]

Results from all three studies are consistent with our general concepts of shield behavior and neutron spectral distribution when high-energy accelerator-produced particles generate the radiation field. We see that the various threshold detectors are quite effective in providing information for investigating such phenomena, and that lack of basic nuclear-reaction data is one of the most serious limitations to more widespread and effective use of these detectors.

ACKNOWLEDGEMENTS

Much of the information presented here represents the work of others at this Laboratory, both within and without the Health Physics Department.

Formal contributions are acknowledged in the accompanying list of references; however, informal contributions probably outweigh the listed ones in importance. Among the outstanding items in the latter category for which we give especial thanks are:

J. B. McCaslin, A. J. Miller, M. A. Pick, and L. D. Stephens, for radiation survey and threshold detector data taken at the Bevatron;

H. S. Dakin, for radiation survey data taken at large distances from the Bevatron;

N. Horowitz, B. J. Moyer, H. W. Patterson, R. Wallace, and T. Zipf, for participation on an informal committee to study requirements for shielding of improved Bevatron;

H. W. Patterson, R. H. Thomas, and R. Wallace, for work in connection with determination of the preferred shape for the Bevatron neutron spectrum;

Mrs. Nickey Little, for acting as our intermediary with the digital computers;

The Bevatron staff, for shield-array construction, beam transport and monitoring, and efficient accelerator operation during the shield-array experiment; also, for their generally helpful and cooperative spirit shown toward all our work at this accelerator;

Particular appreciation is expressed to B. J. Moyer, Administrative Head, Health Physics Department, who originally generated the climate within which the kind of work reported here could be accomplished; such appreciation is also expressed to H. W. Patterson, who has maintained and further encouraged this climate in his supervision of our Health Physics work.

FOOTNOTES AND REFERENCES

*This work was performed under the auspices of the U. S. Atomic Energy Commission.

†For the First Symposium on Accelerator Radiation Dosimetry and Experience, Brookhaven National Laboratory, November 3-5, 1965. To be presented at SESSION III.

1. B. J. Moyer, Evaluation of Shielding Required for the Improved Bevatron, in Proceedings of the Conference on Shielding Near Large Accelerators, Saclay, France, 1962, Presses Universitaires de France, Paris.

2. A. R. Smith, Final Study of Radiation Field Around the Partially Shielded Bevatron, (Health Physics internal report), November 1962 (unpublished).

3. Henry S. Dakin (Lawrence Radiation Laboratory), private communication and department files.

4. J. B. McCaslin, A High Energy Neutron Dosimeter, Health Physics 2 : 399-407 (1960).

5. J. C. Ringle, A Technique for Measuring Neutron Spectra in the Range 2.5 to 30 MeV Using Threshold Detectors (Ph. D. Thesis), Lawrence Radiation Laboratory Report UCRL-10732, October 1963.

6. A. D. Kohler, Jr., An Improved Method of Neutron Spectroscopy Using Threshold Detectors (M. S. Thesis), Lawrence Radiation Laboratory Report UCRL-11760, December 1964.

7. Alan R. Smith, Threshold Detector Applications to Neutron Spectroscopy at the Berkeley Accelerators: Presented at Session II of the First Symposium on Accelerator Radiation Dosimetry and Experience, Brookhaven National Laboratory, November 3-5, 1965.

8. A. R. Smith, J. B. McCaslin, and M. A. Pick, Radiation Field Inside a Thick Concrete Shield for 6.2 BeV Incident Protons, Lawrence Radiation Laboratory Report UCRL-11331, September 1964.

9. W. N. Hess, H. W. Patterson, and R. Wallace, Delay-Line Chamber Has Large Area, Low Capacitance, Nucleonics 15(3): 74-79 (1957).

10. W. N. Hess, H. W. Patterson, R. Wallace, and E. L. Chupp, The Cosmic Ray Neutron Energy Spectrum, Phys. Rev. 116 : 445-457 (1959).

11. H. W. Patterson, W. N. Hess, B. J. Moyer, and R. Wallace, The Flux and Spectrum of Cosmic-Ray Produced Neutrons as a Function of Altitude, Health Physics 2(1) : 69-72 (1959).

12. J. Baarli, (CERN) private communication, March 1965.

13. C. Distenfeld, (Brookhaven National Laboratory) private communication, June 1965.

14. R. Sanna, K. O'Brien, M. Alberg, S. Rothenberg, and J. McLaughlin, Nuclear Emulsion Spectrometry at Low and Intermediate Neutron Energies, AEC Health and Safety Laboratory Report HASL-162, July 1965.

15. H. A. Wollenberg and A. R. Smith, A Concrete Low-Background Counting Enclosure, Lawrence Radiation Laboratory Report UCRL-11454, June 1964; and Health Physics (to be published).

16. H. W. Patterson, The Effect of Shielding on Radiation Produced by the 730 MeV Synchrocyclotron and the 6.3 GeV Proton Synchrotron at the Lawrence Radiation Laboratory, in Proceedings of the Conference on Shielding Near Large Accelerators, Saclay, France, 1962, Presses Universitaires de France, France.

17. R. G. Alsmiller, Jr., and J. E. Murphy, Nucleon-Meson Cascade Calculations: The Star Density Produced by a 24-GeV Proton Beam in Heavy Concrete, Oak Ridge National Laboratory ORNL-3367 (1963).

18. R. J. Riddell, High Energy Nuclear Cascades Lawrence Radiation Laboratory UCRL-11989, 1963 (unpublished).

FIGURE CAPTIONS UCRL-16323

Fig. 1. Photograph of Bevatron, 1960, showing ring shield, open top, tangent-tank roof shields, and partial installation of some wood shielding.

Fig. 2. Photograph of Bevatron, early 1963, showing new ring shield in place and partially completed new roof shield.

Fig. 3. Elevation view of Bevatron showing relationship of crane walkway to shield and accelerator structure.

Fig. 4. Shield-evaluation data: neutron flux profiles measured along crane walkway in 1965, after shield improvement.

Fig. 5. Shield-evaluation data: neutron flux profiles measured along crane walkway in 1962, before shield improvement.

Fig. 6. Plan view of shield array.

Fig. 7. Working face of shield array.

Fig. 8. Detectors positioned in wooden troughs.

Fig. 9. Beam-axis attenuation profiles for carbon, aluminum, and gold.

Fig. 10a. Lateral-attenuation profiles for gold-foil detector.

Fig. 10b. Lateral-attenuation profiles for aluminum detector.

Fig. 10c. Lateral-attenuation profiles for carbon detector.

Fig. 11a. Constant-attenuation profiles for gold-foil detector.

Fig. 11b. Constant-attenuation profiles for aluminum detector.

Fig. 11c. Constant-attenuation profiles for carbon detector.

Fig. 12a. Constant-flux contours for gold-foil detector.

Fig. 12b. Constant-flux contours for aluminum detector.

Fig. 12c. Constant-flux contours for carbon detector.

Fig. 13a. Attenuation profiles at several angles for gold-foil detector.

Fig. 13b. Attenuation profiles at several angles for aluminum detector.

Fig. 13c. Attenuation profiles at several angles for carbon detector.

Table 1. Summary of craneway data, 1962 and 1965 studies.

	Moderated Au foils	Aluminum disks
1965 Avg n/cm^2 sec at 2.3×10^{12} p+/pulse	18.2	1.08
1965 Avg n/cm^2 sec at 1.0×10^{11} p+/pulse	0.78	0.0465
1962 Avg n/cm^2 sec at 1.0×10^{11} p+/pulse	337	4.21
Ratio $\frac{1962 \text{ avg}}{1965 \text{ avg}}$ (shield-improvement factor)	432	90.5

Table 2. Step-function solution values for Bevatron shield neutron spectra.

Energy Interval (MeV)	$\phi(E)$ for Fig. 16 4'-1'	$\phi(E)$ for Fig. 16 4'-3'	$\phi(E)$ for Fig. 17 8'-2'	$\phi(E)$ for Fig. 17 8'-4'
2-6	2.38×10^{6}	2.78×10^{5}	3.0×10^{5}	5.9×10^{4}
6-11	0.57×10^{6}	0.65×10^{5}	0.65×10^{5}	1.25×10^{4}
11-16	0.50×10^{6}	0.37×10^{5}	0.37×10^{5}	0.65×10^{4}
16-22	0.24×10^{5}	0.24×10^{5}	0.24×10^{5}	0.58×10^{4}
22-30	0.21×10^{6}	0.16×10^{5}	0.21×10^{5}	0.50×10^{4}

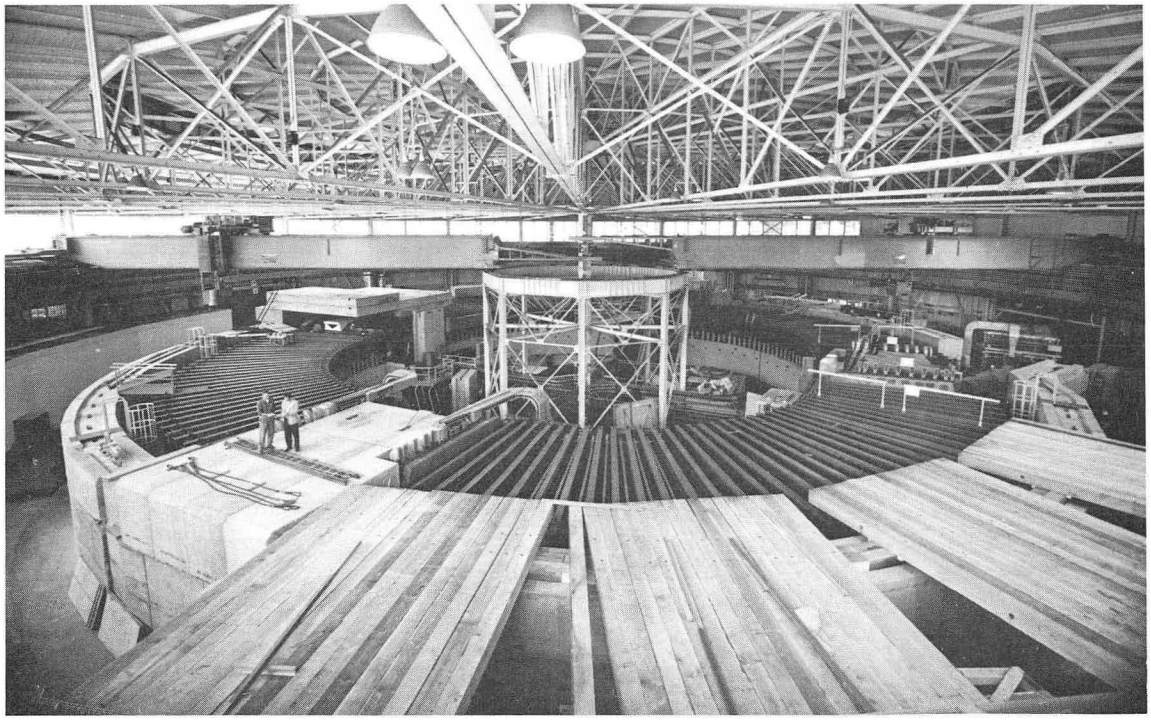

ZN-5254

Fig. 1

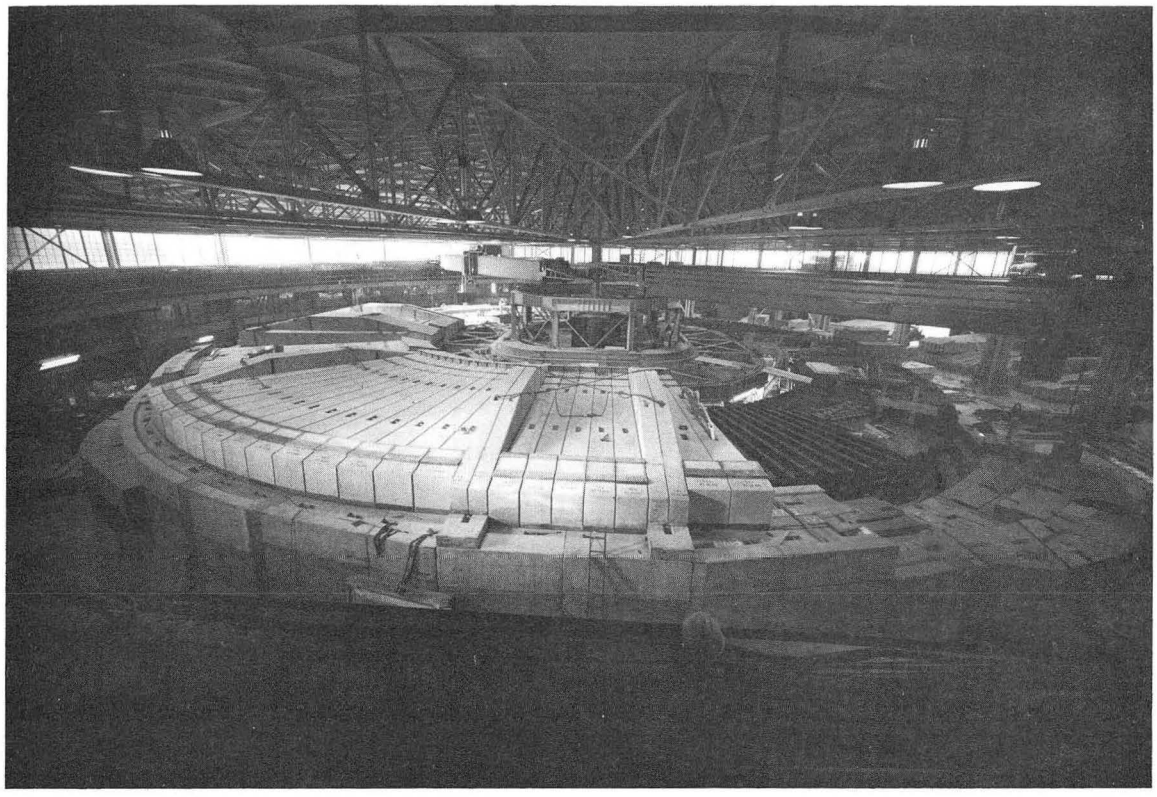

ZN-4100

Fig. 2

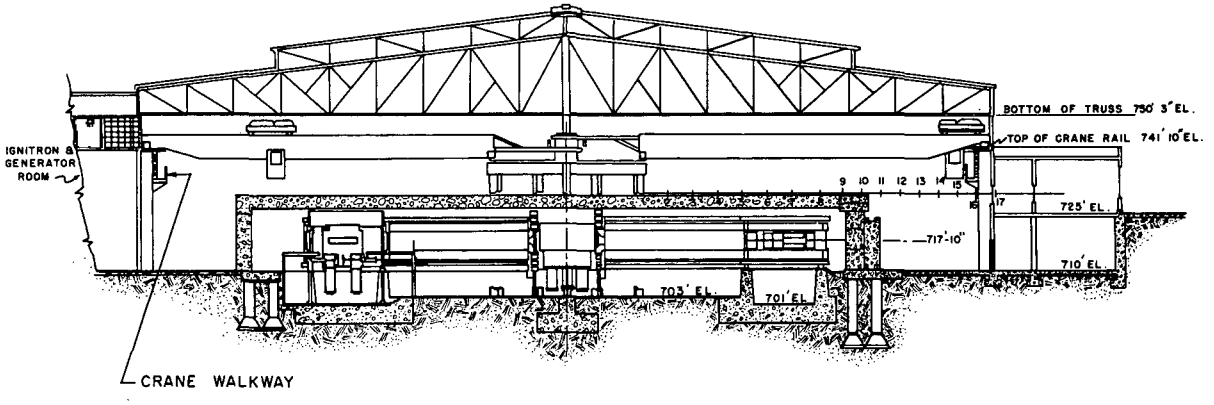

MUB-8464

Fig. 3

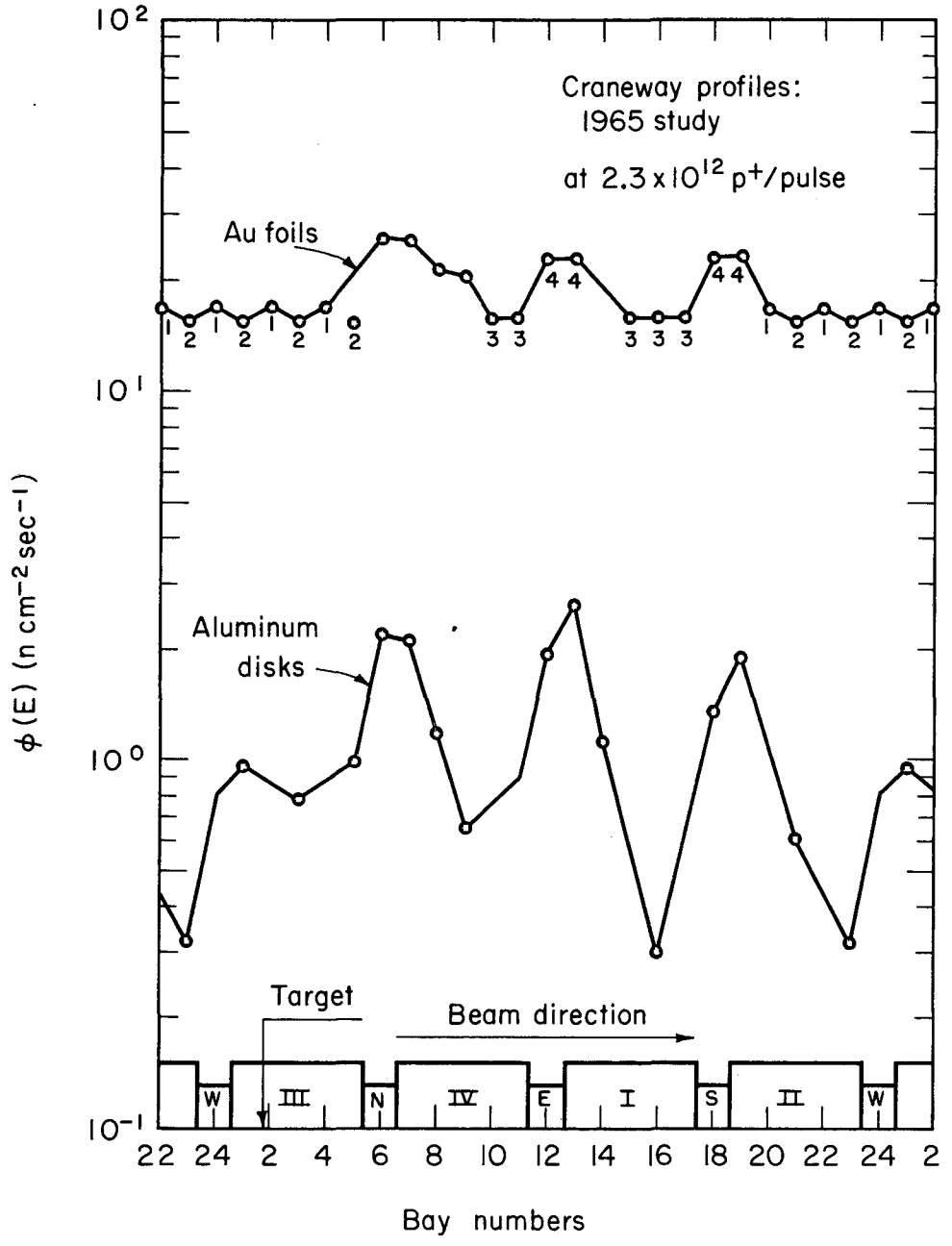
Craneway profiles:
1965 study
at 2.3 x 10^12 p+/pulse
Au foils
Aluminum
disks
Target
Beam direction
W
III
N
IV
E
I
S
II
W
φ(E) (n cm^-2 sec^-1)
Bay numbers
MUB-8446

Fig. 4

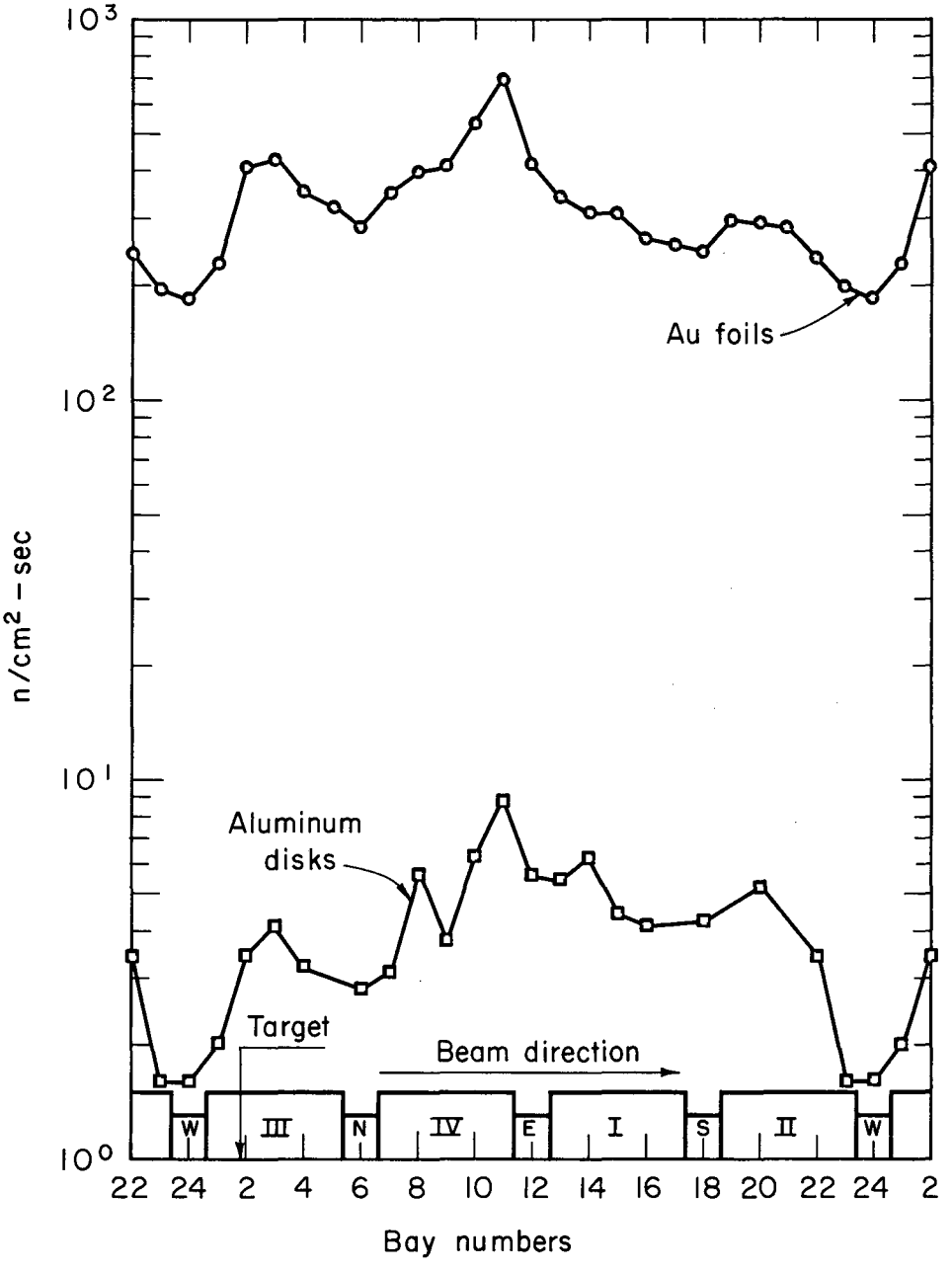

MUB-8447

Fig. 5

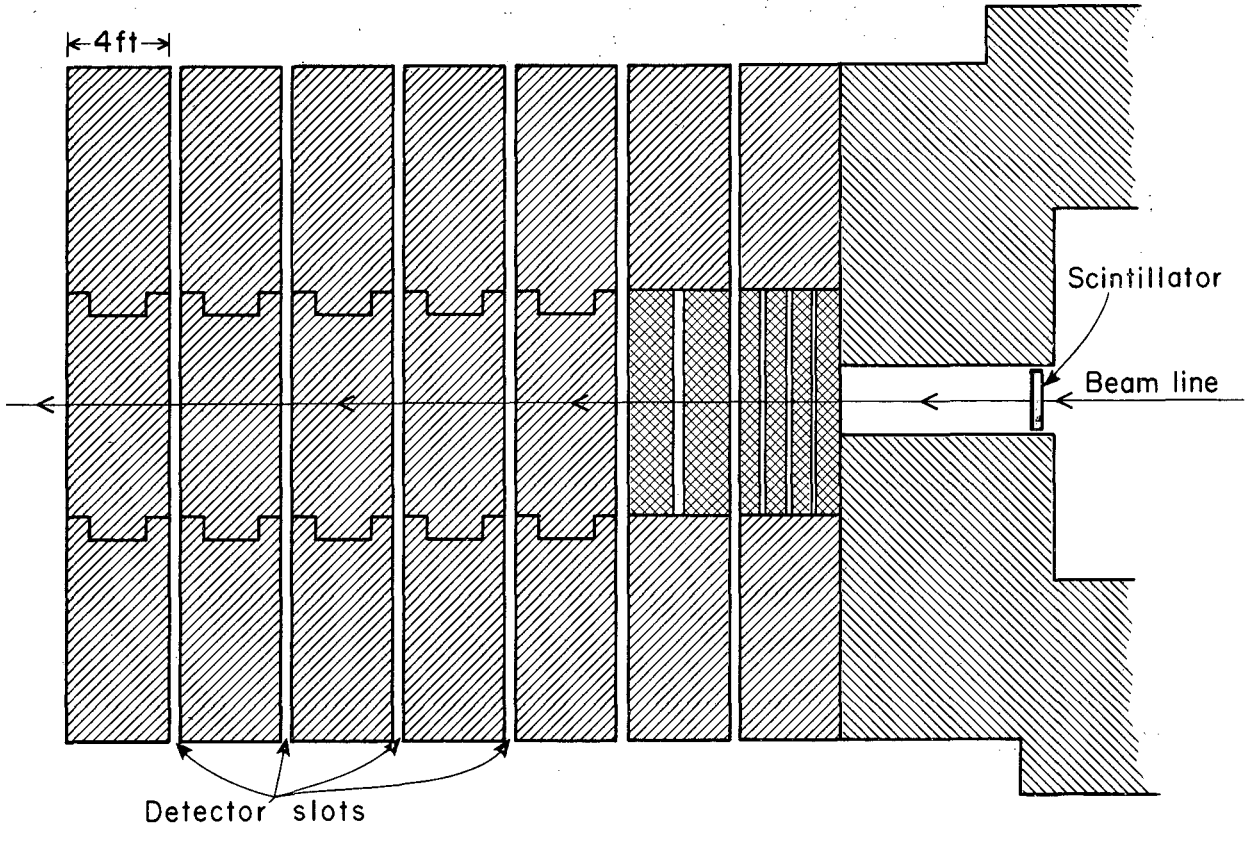

MUB-3055

Fig. 6

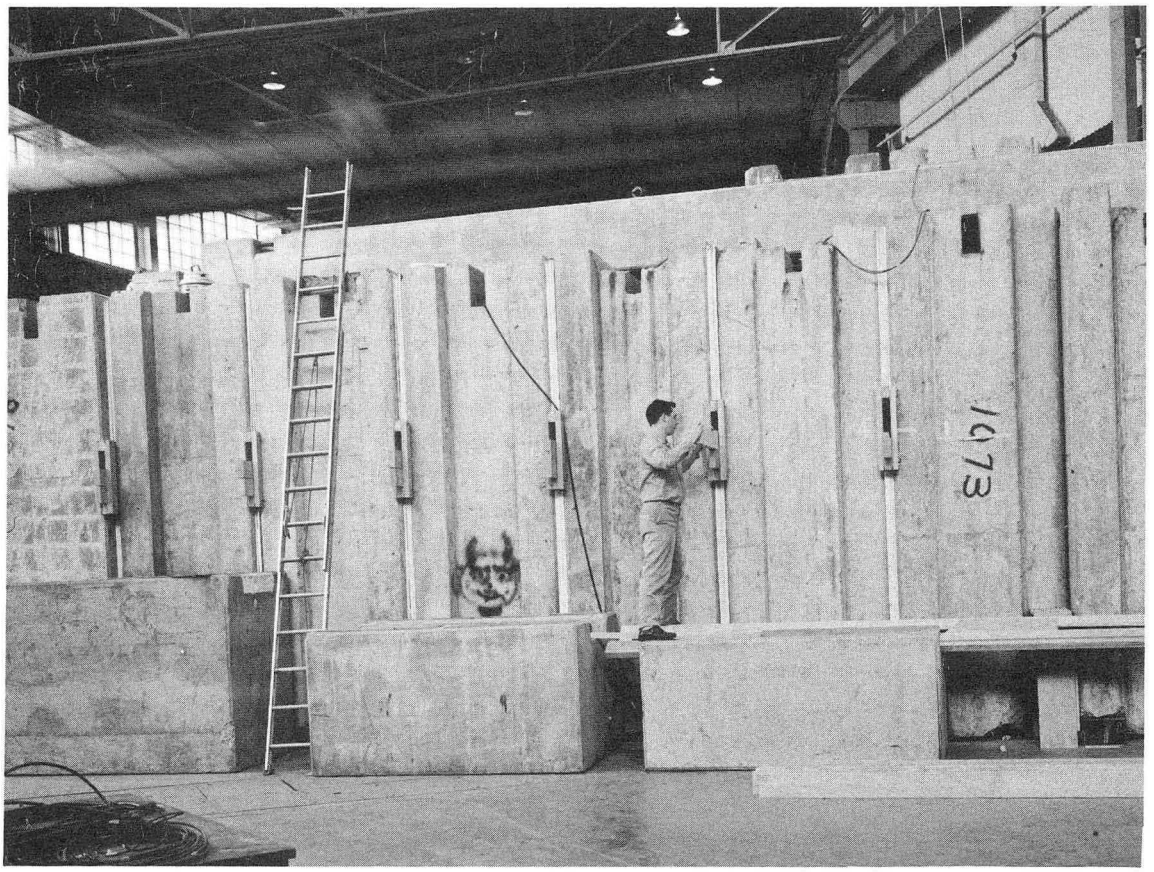

ZN-4498

Fig. 7

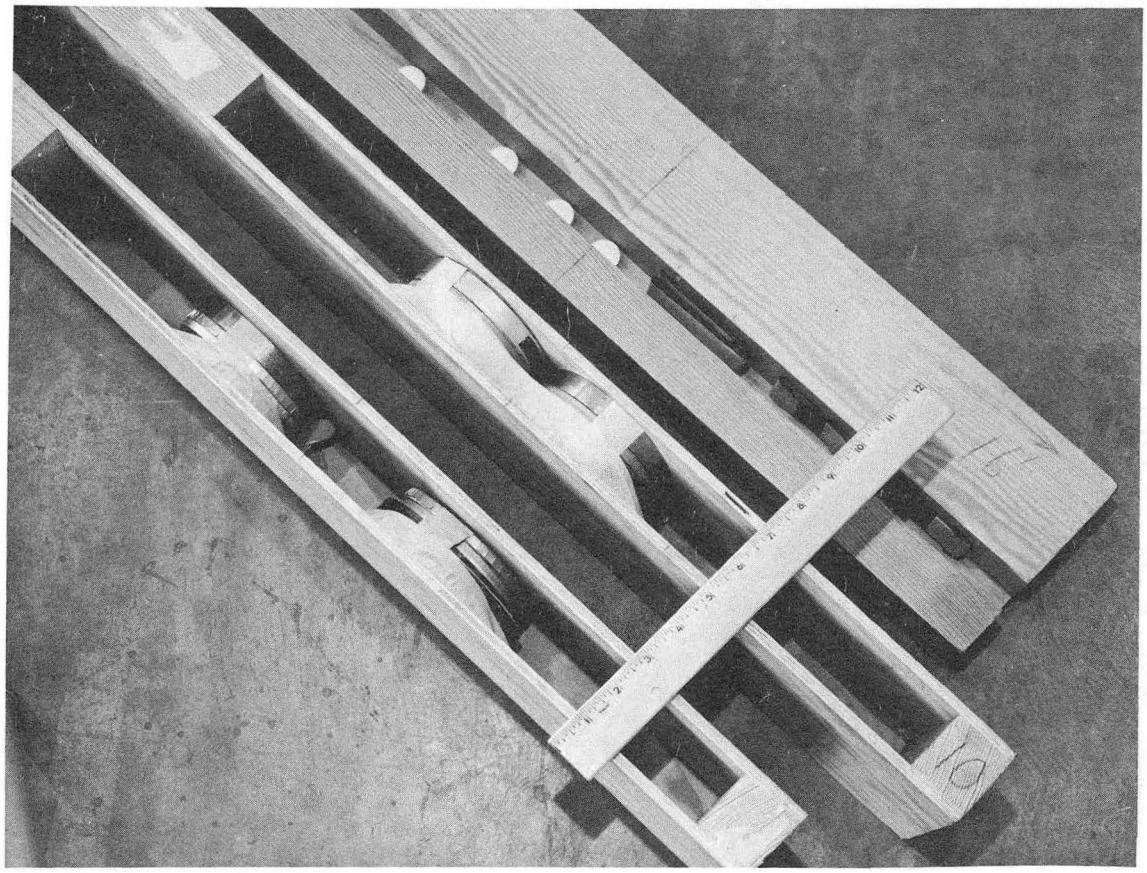

ZN-4499

Fig. 8

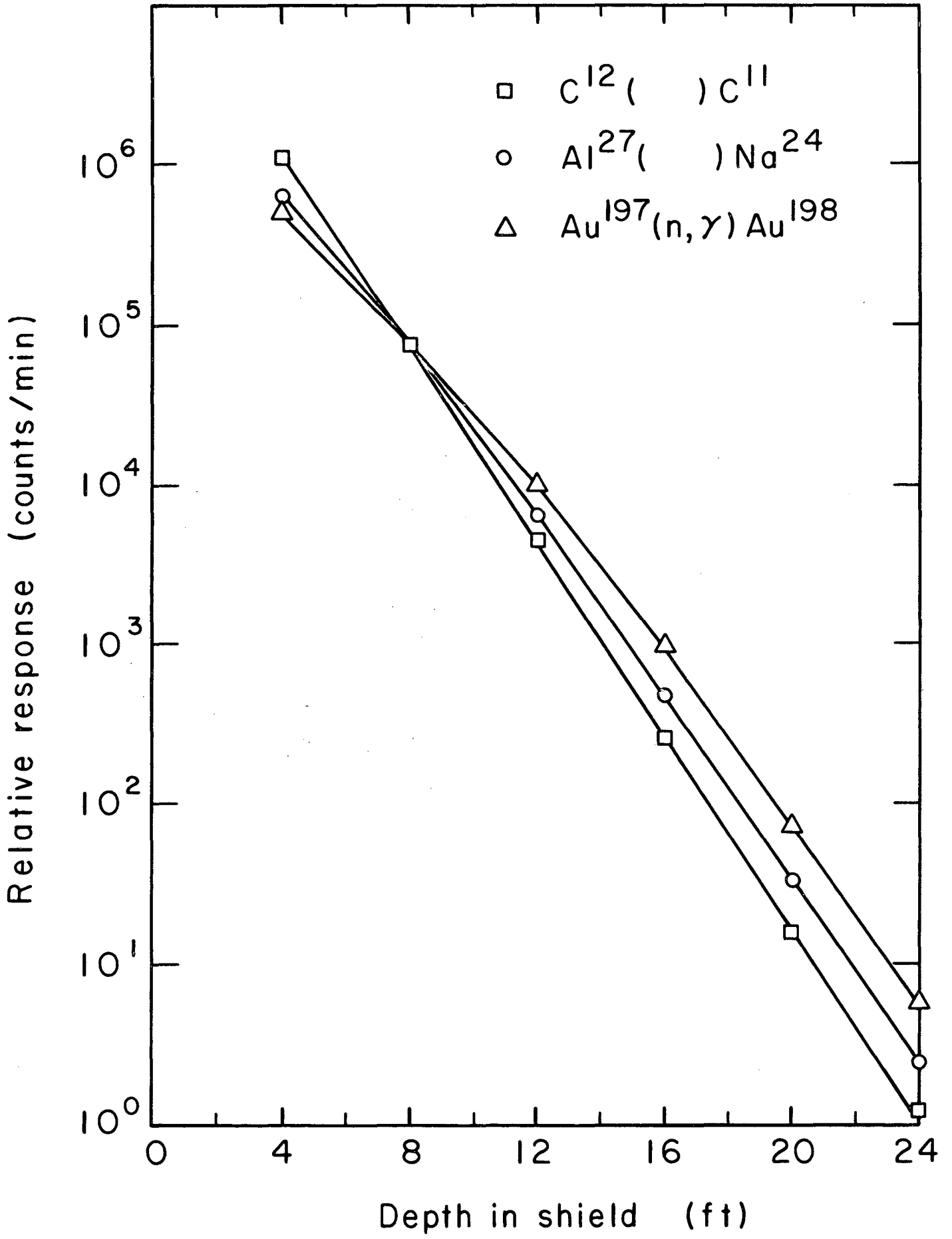

Fig. 9 Beam-axis attenuation profiles for carbon, aluminum, and gold

MUB-3056 -A

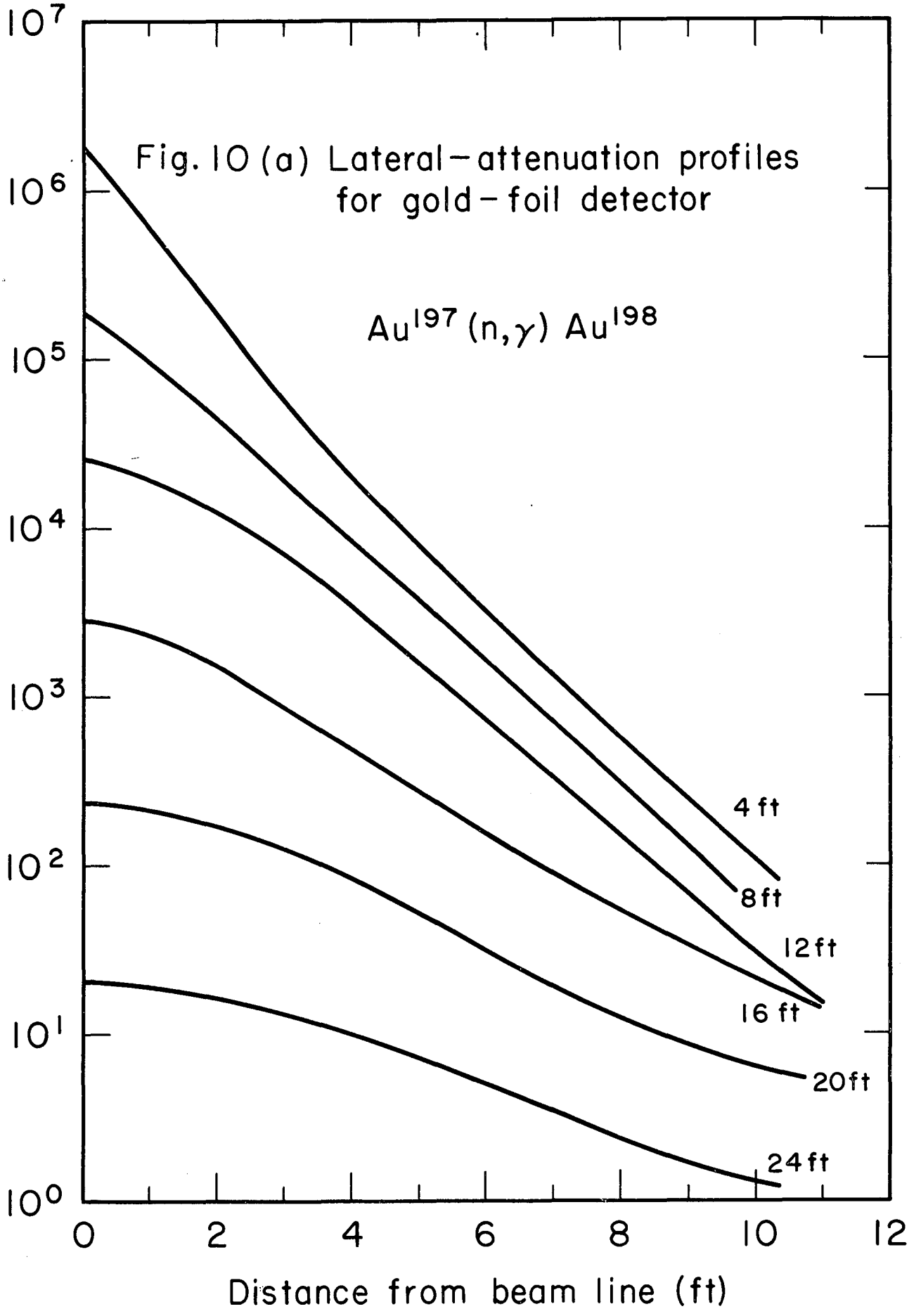
Fig. 10 (a) Lateral-attenuation profiles for gold-foil detector
$Au^{197}(n,\gamma)\ Au^{198}$
10^7
10^6
10^5
10^4
10^3
10^2
10^1
10^0
4 ft
8 ft
12 ft
16 ft
20 ft
24 ft
0
2
4
6
8
10
12
Distance from beam line (ft)

MUB-4044

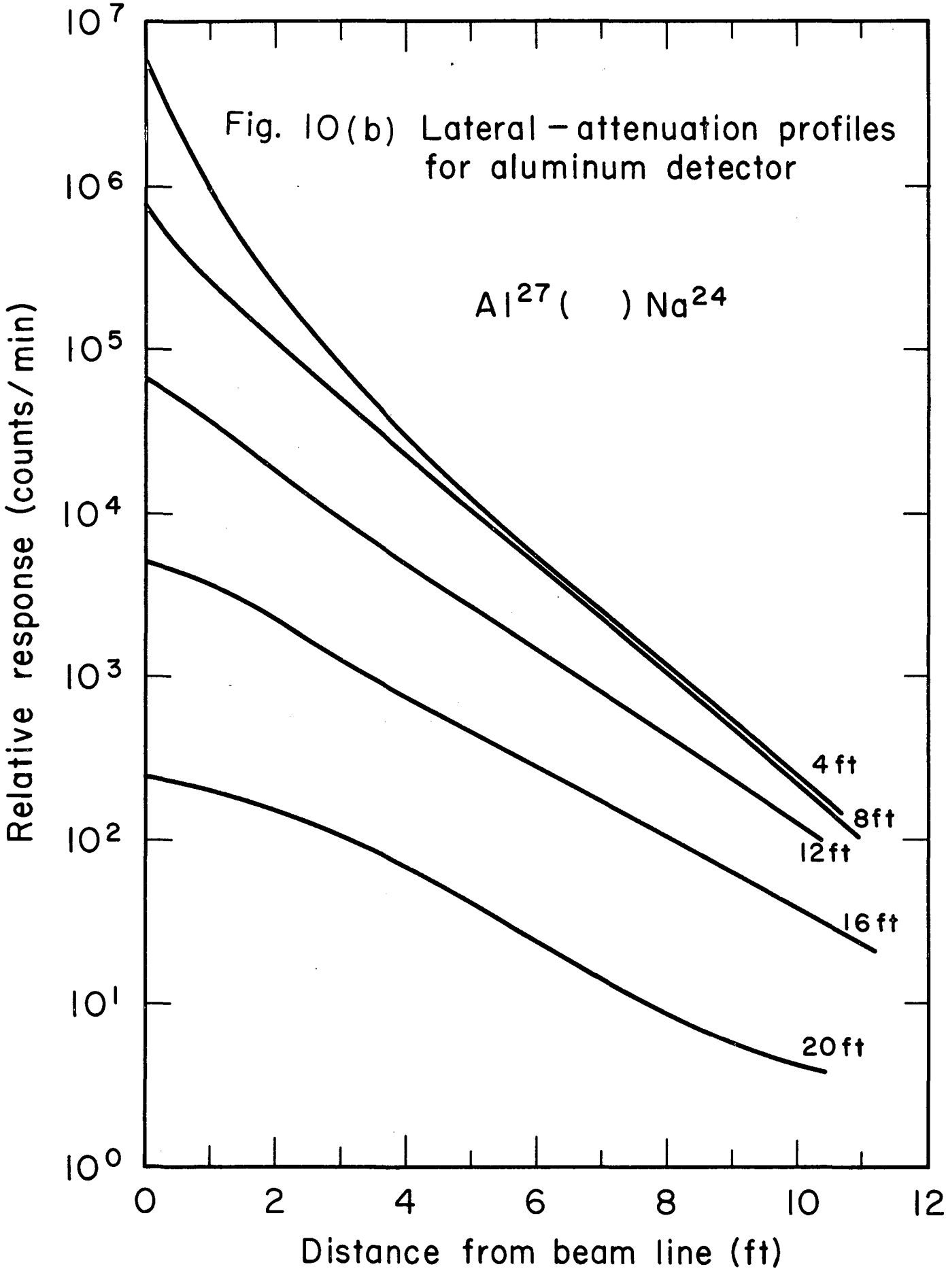
Fig. 10(b) Lateral-attenuation profiles for aluminum detector
Al^{27}( ) Na^{24}
Relative response (counts/min)
10^7
10^6
10^5
10^4
10^3
10^2
10^1
10^0
4ft
8ft
12ft
16ft
20ft
0
2
4
6
8
10
12
Distance from beam line (ft)

MUB-4045

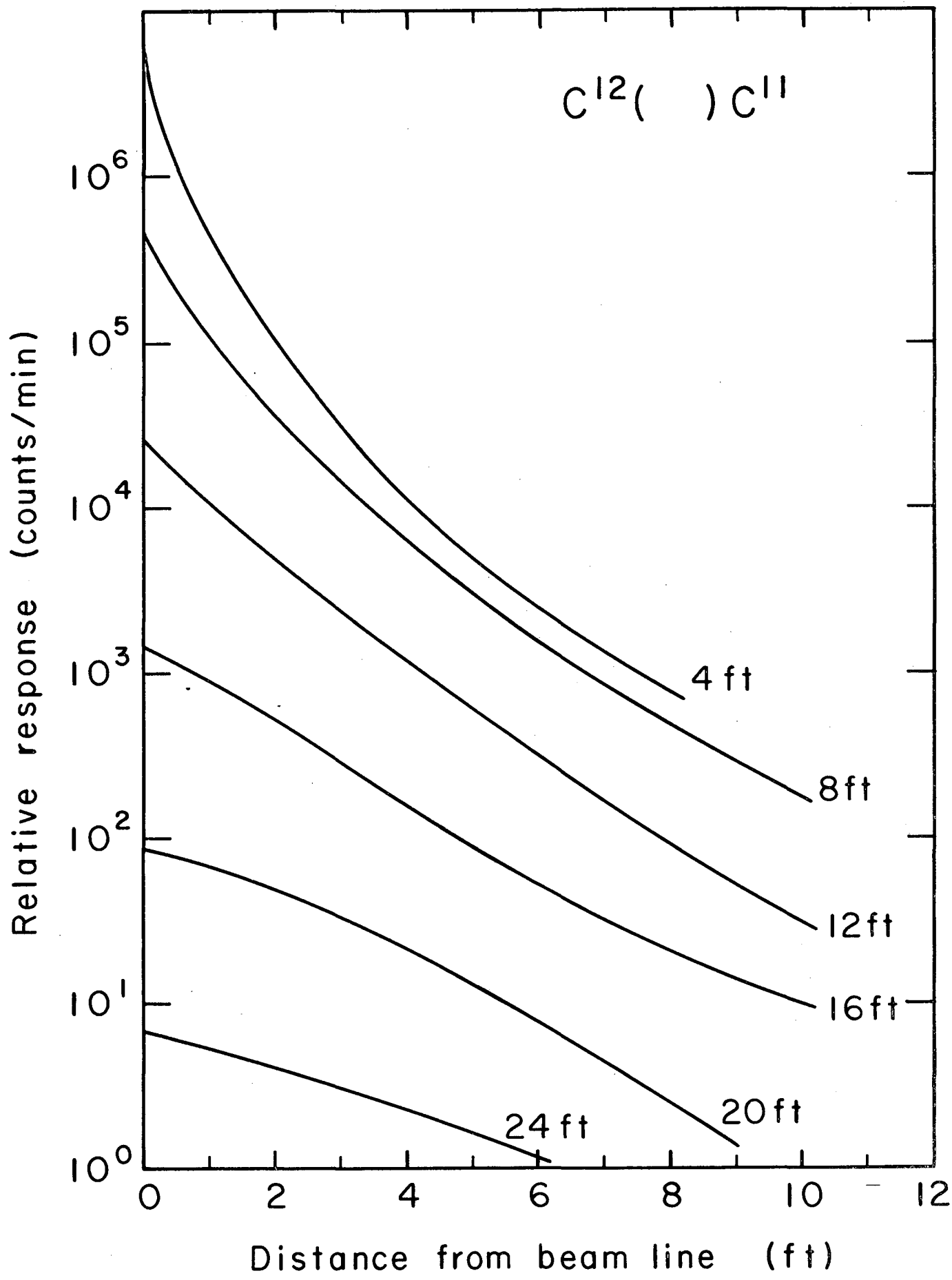

Fig. 10(c) Lateral-attenuation profiles for carbon detector

MUB-3057 -A

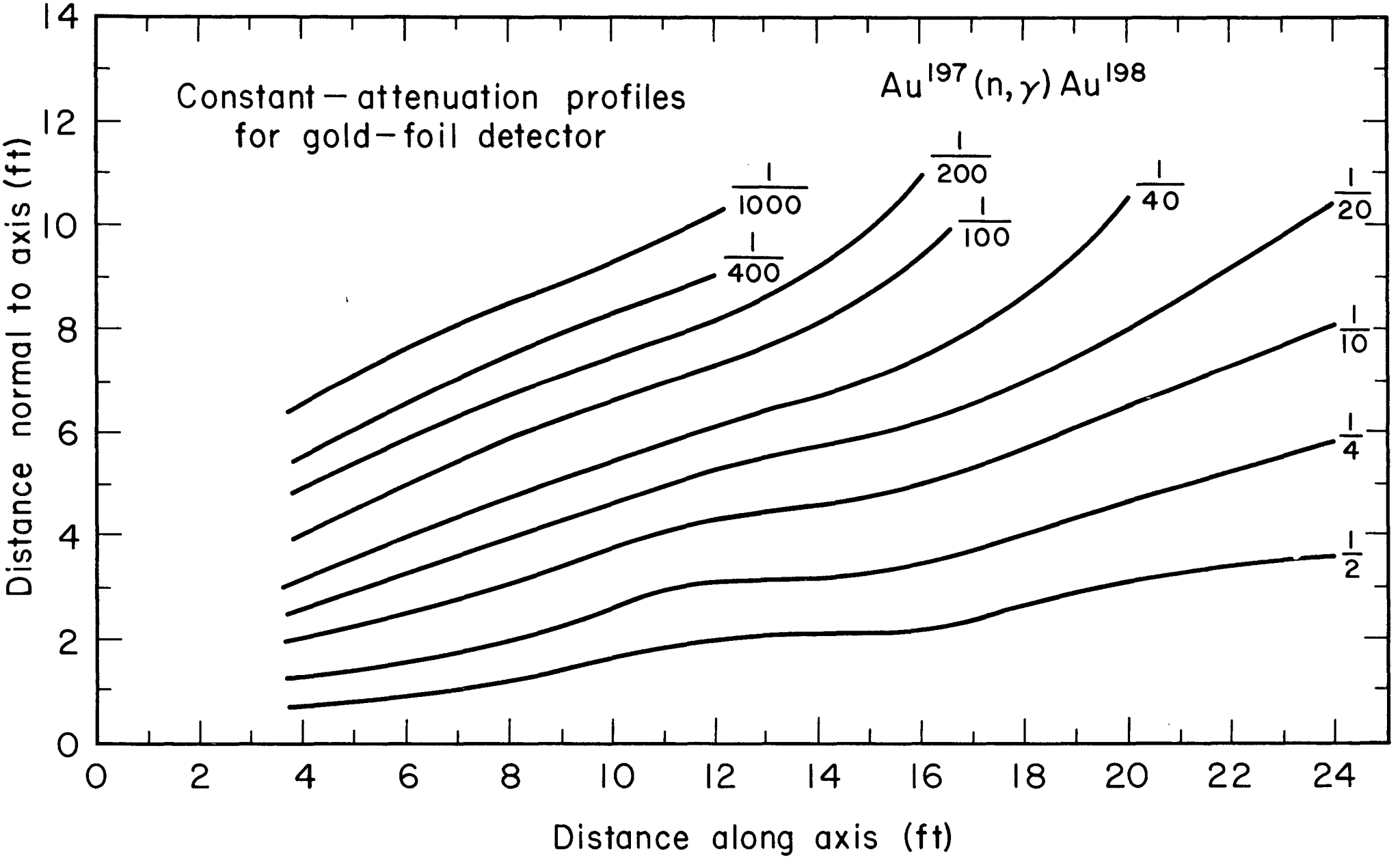

Fig. 11 (a)

MUB-4046

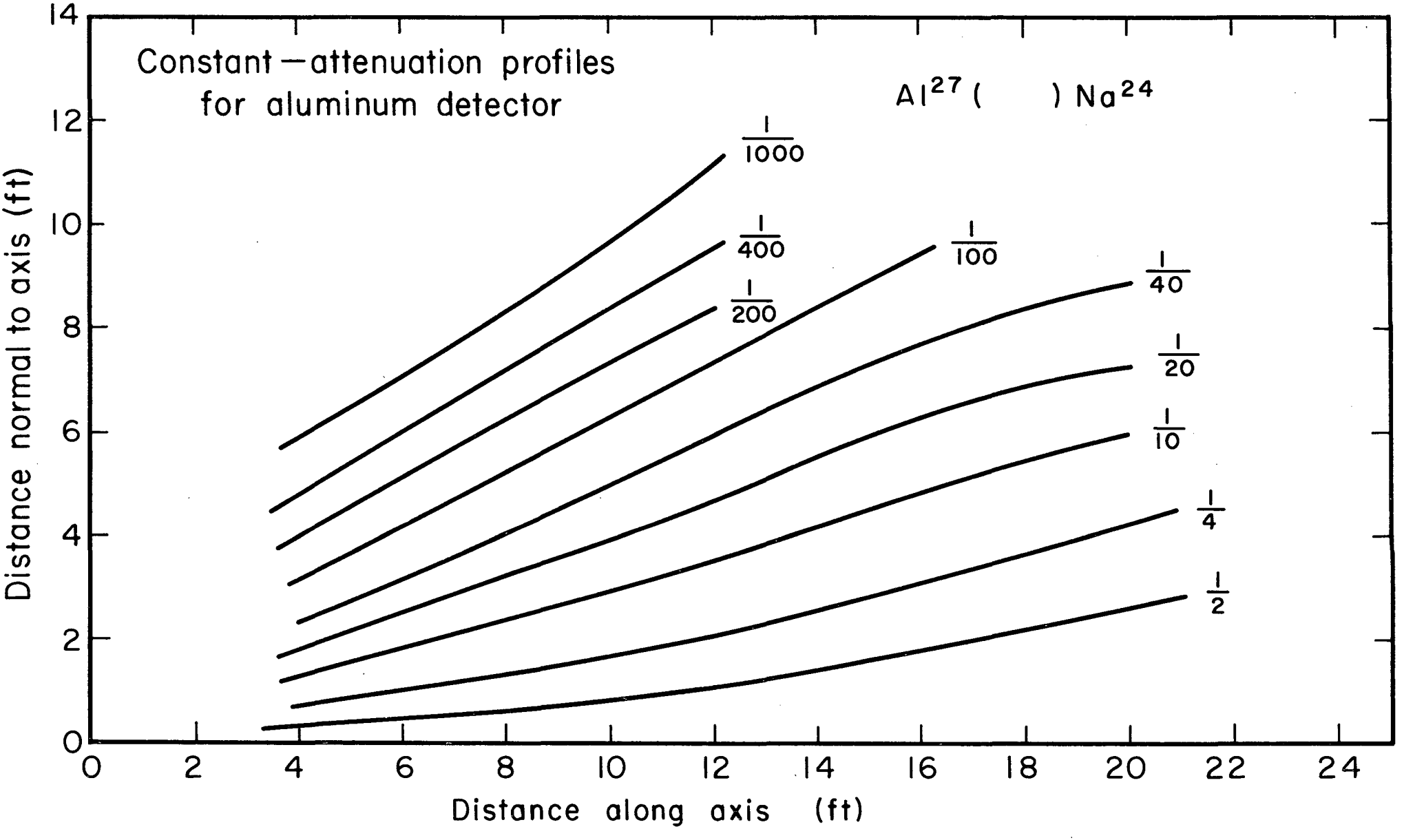

Fig. 11(b)

MUB-4047

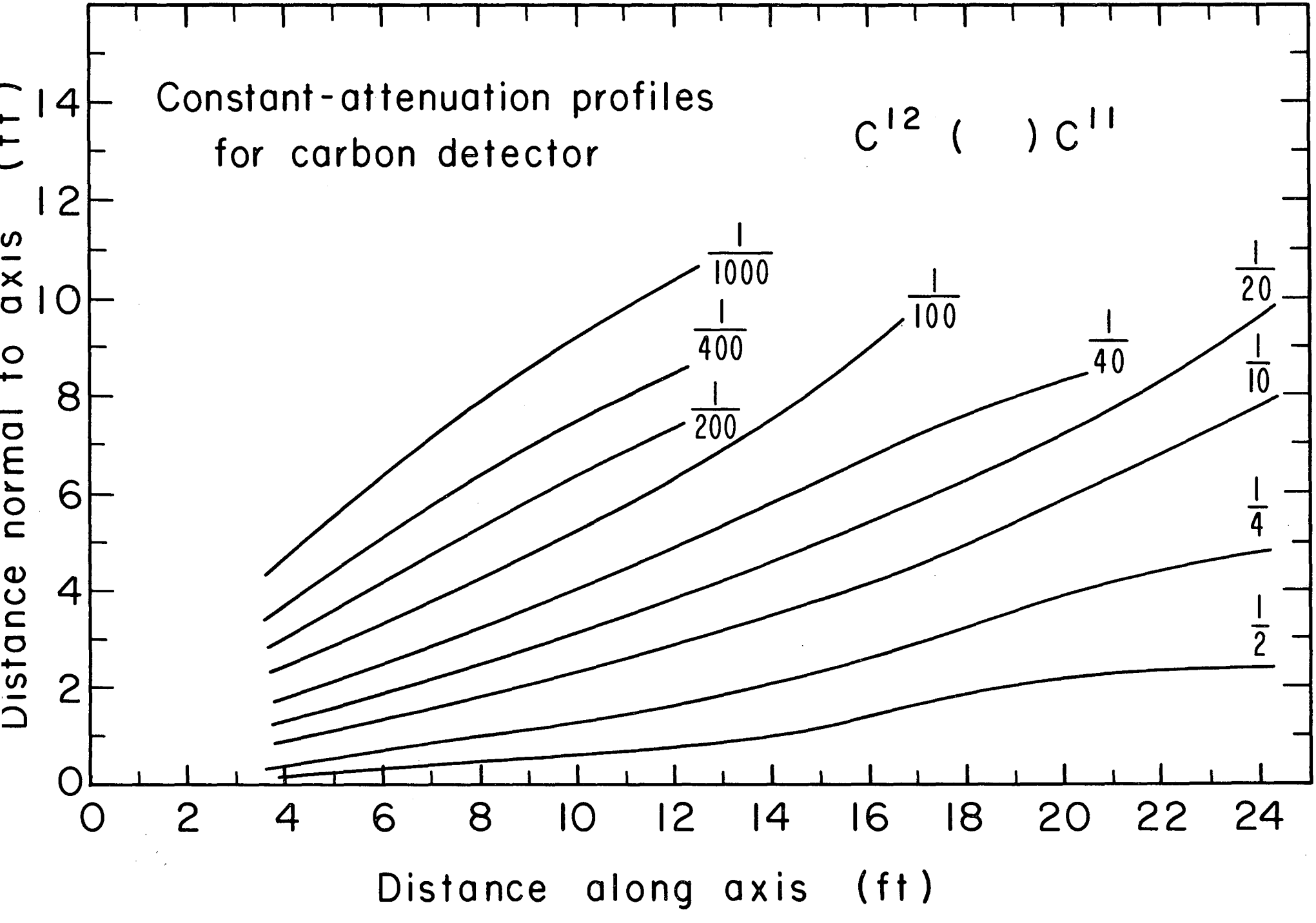

Fig. 11(c)

MUB-3058 -A

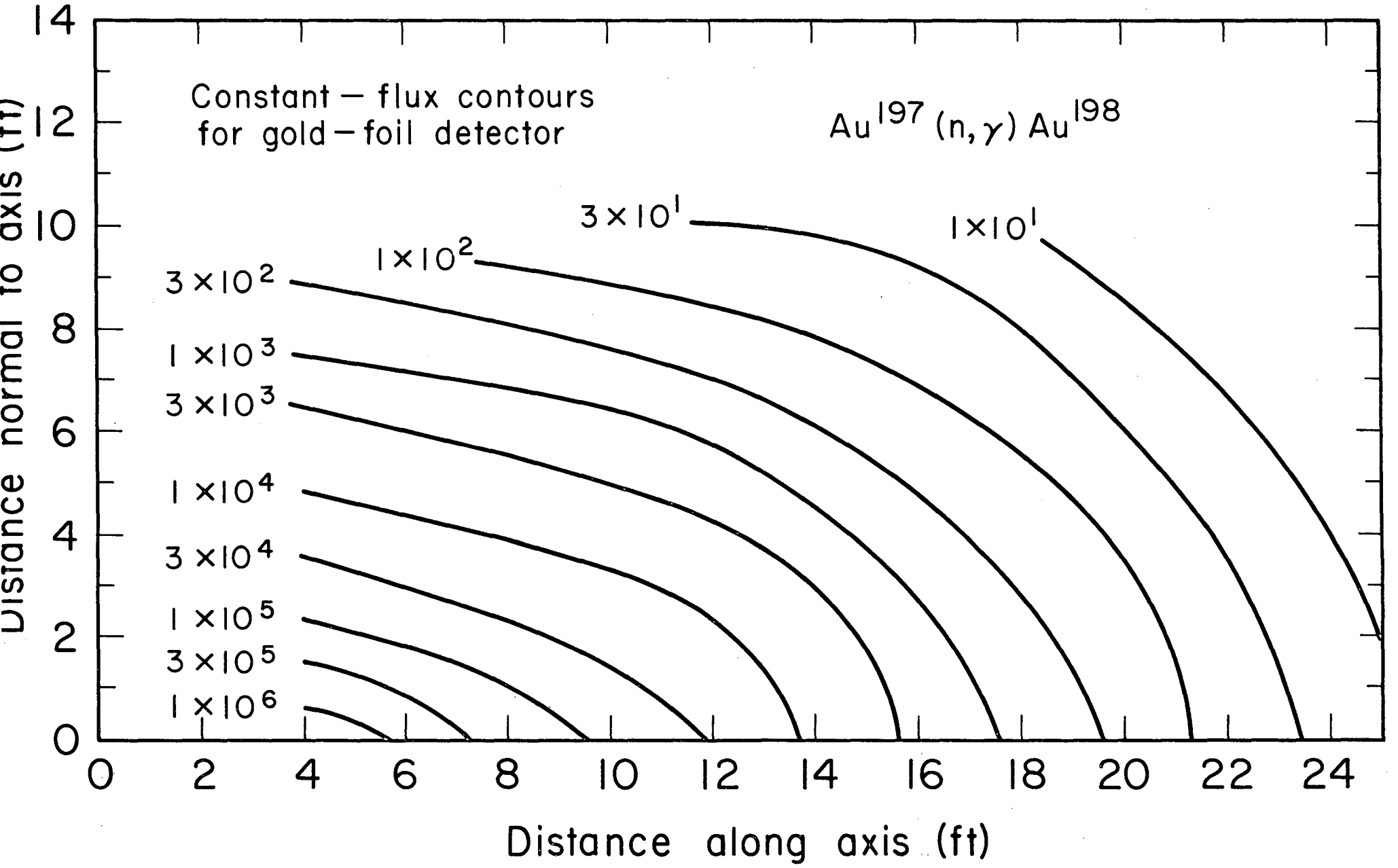

Fig. 12 (a)

MUB-4048

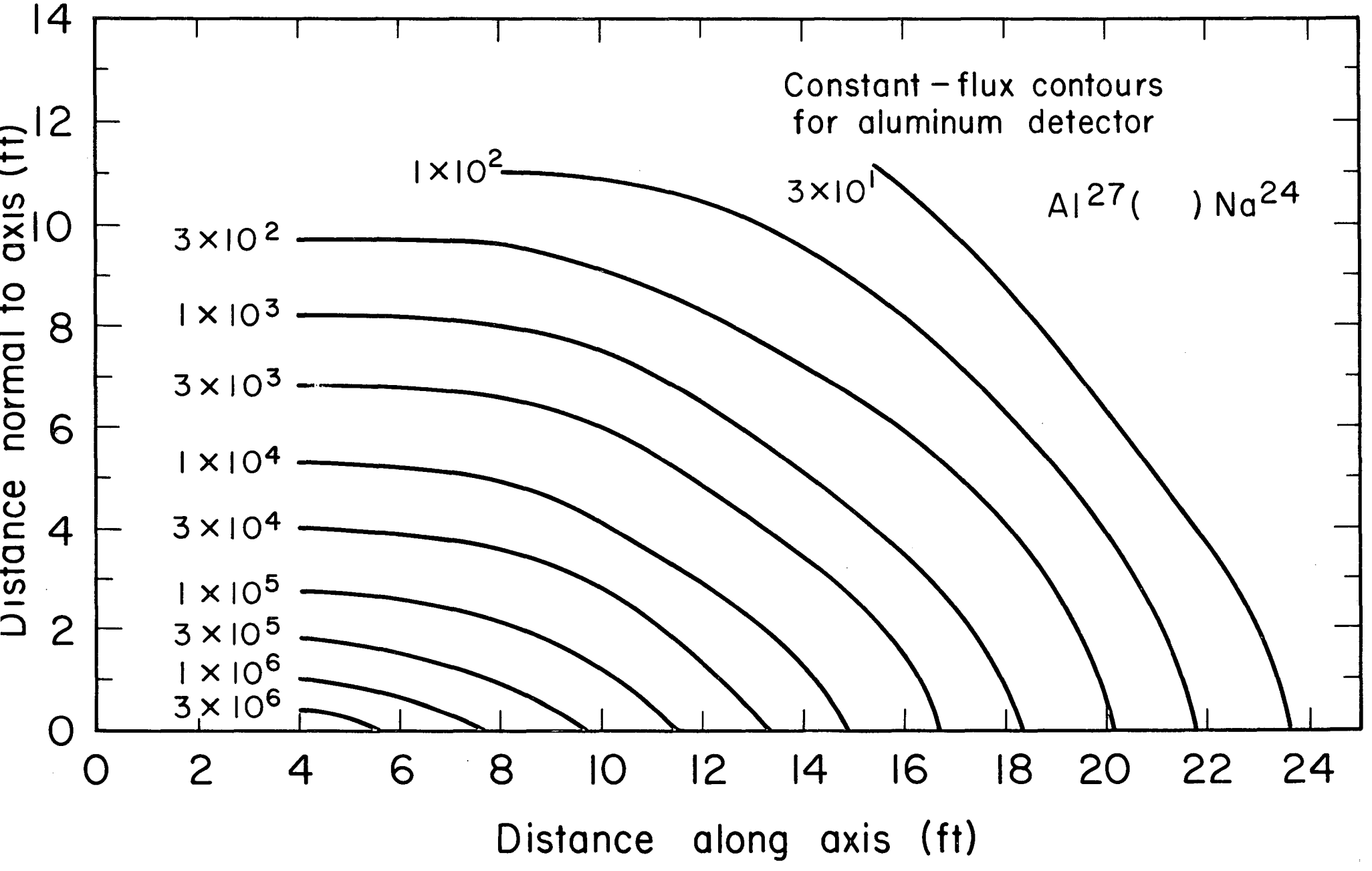

Fig. 12 (b)

MUB-4049

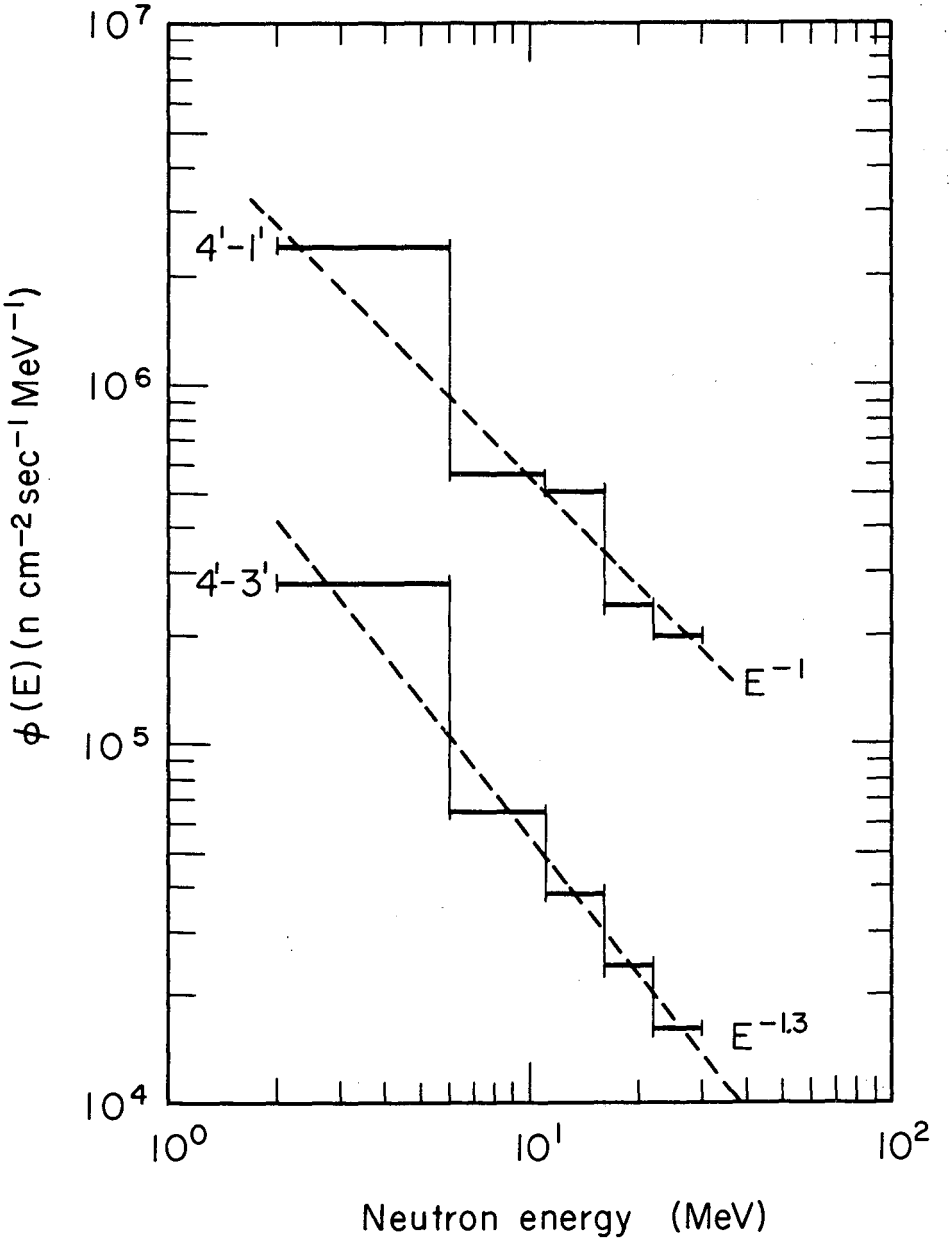

MUB-8450

Fig. 16

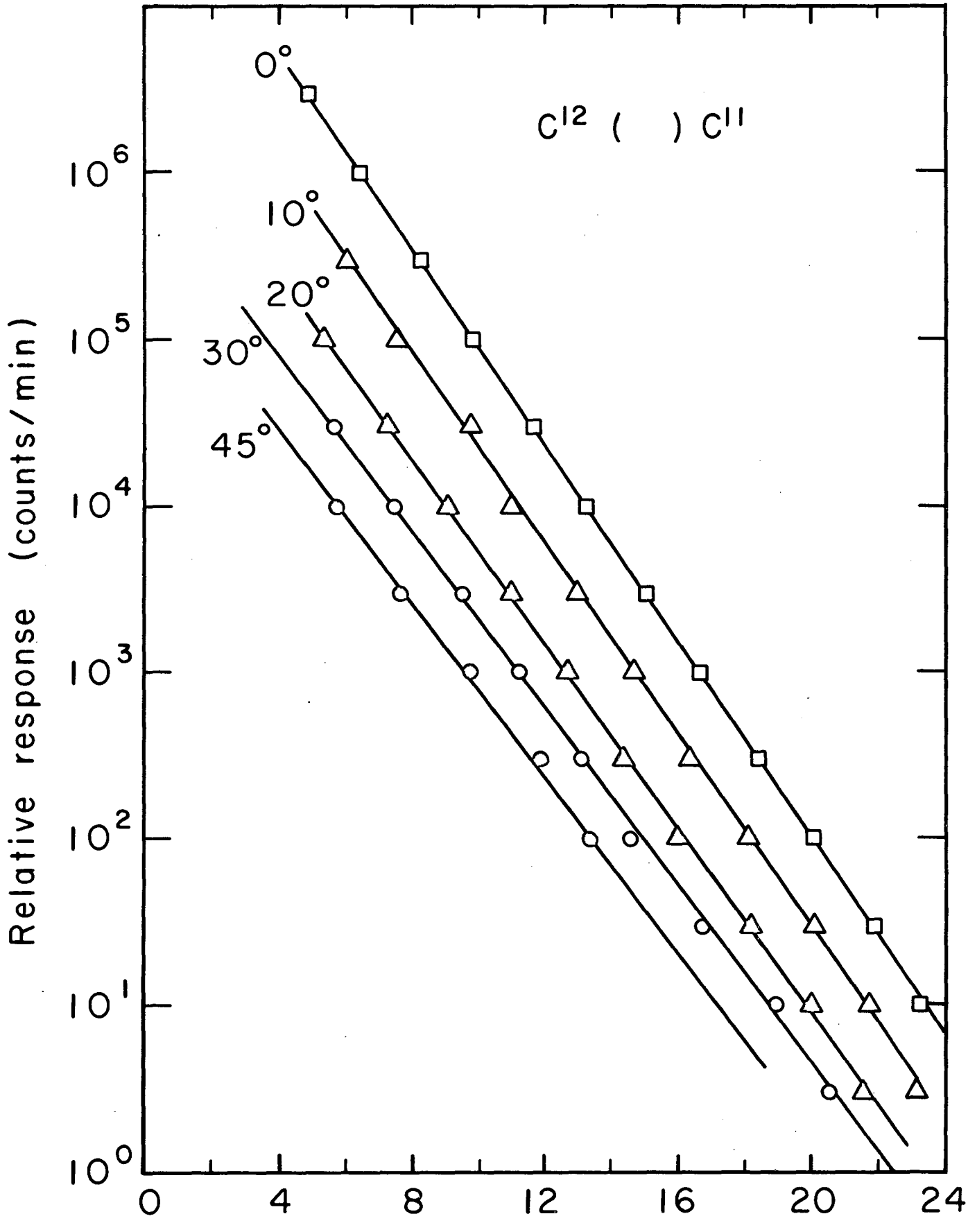

Fig. 13(c) Attenuation profiles at several angles for carbon detector

MUB-3060 -A

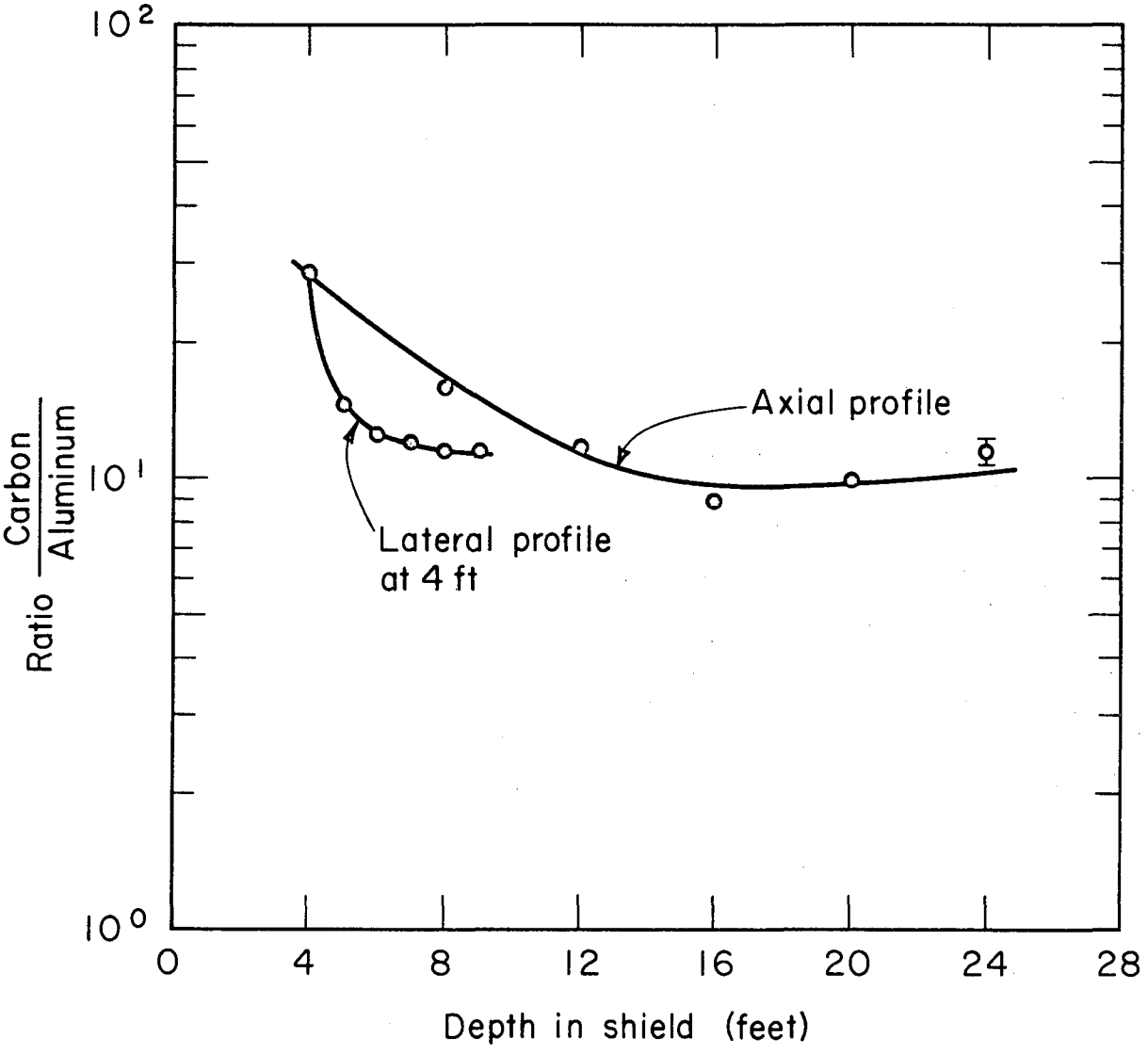
10^2
10^1
10^0
Ratio Carbon / Aluminum
Axial profile
Lateral profile at 4 ft
0
4
8
12
16
20
24
28
Depth in shield (feet)
MUB-8448

Fig. 14

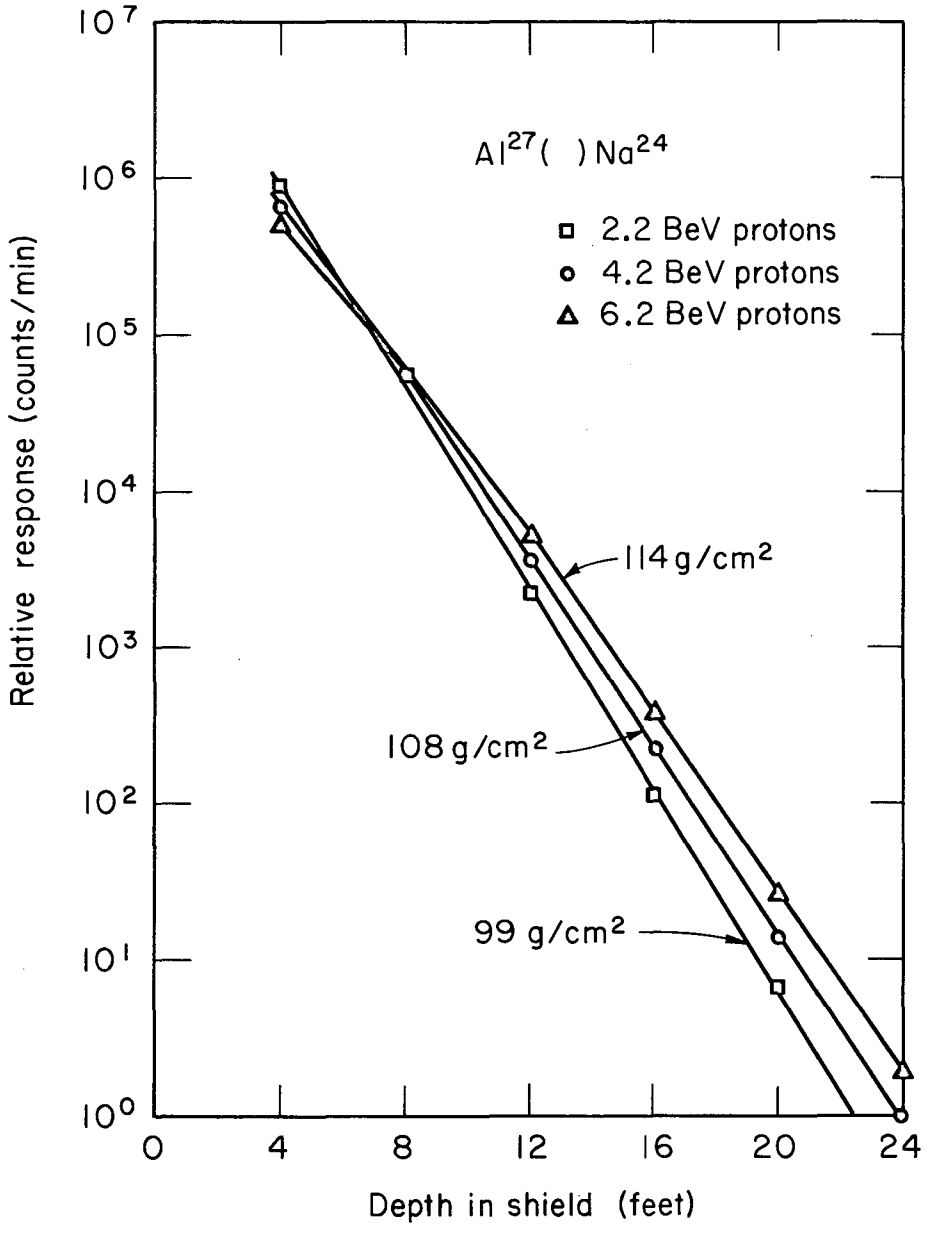

MUB-8449

Fig. 15

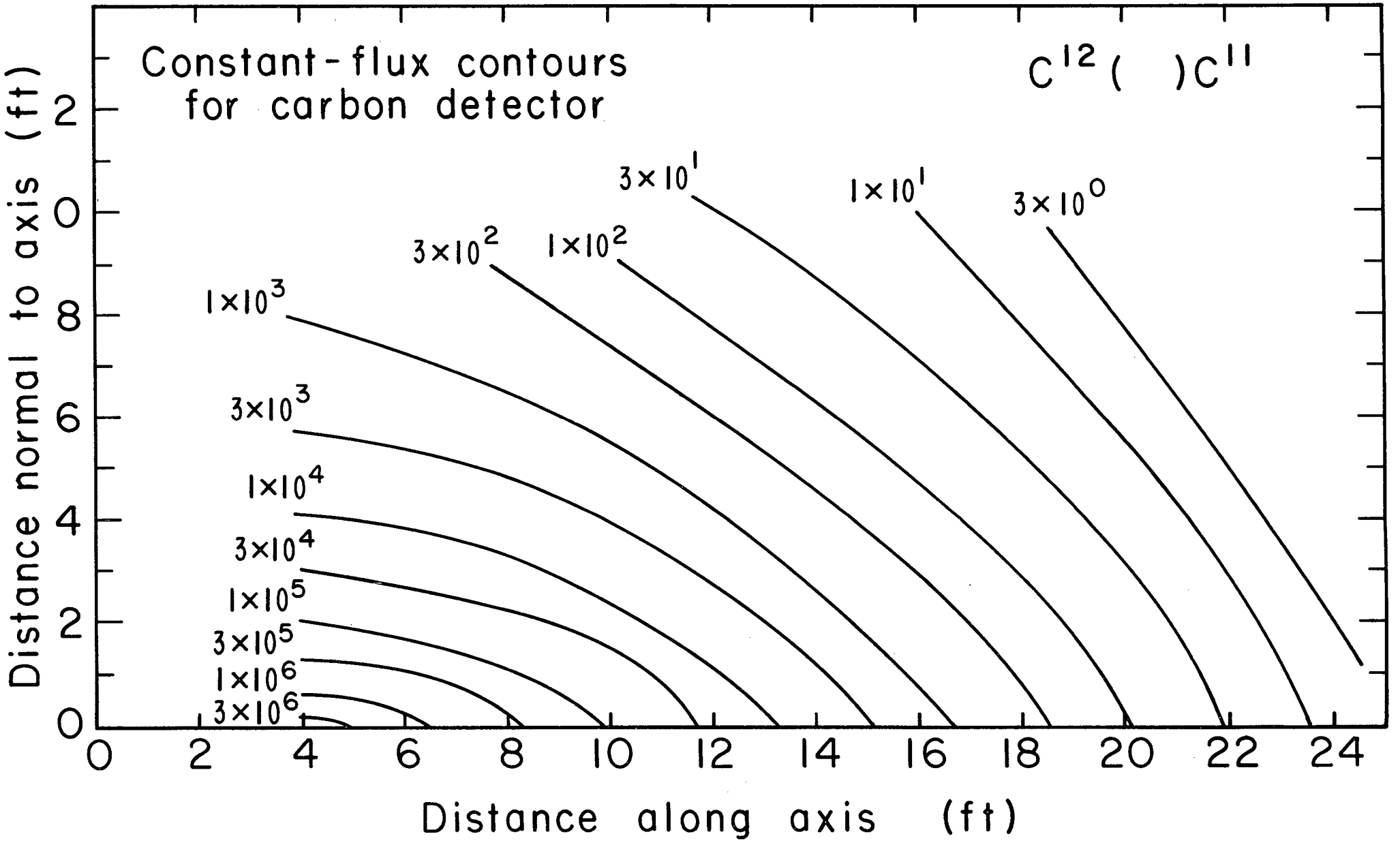

Fig. 12(c)

MUB-3059 -A

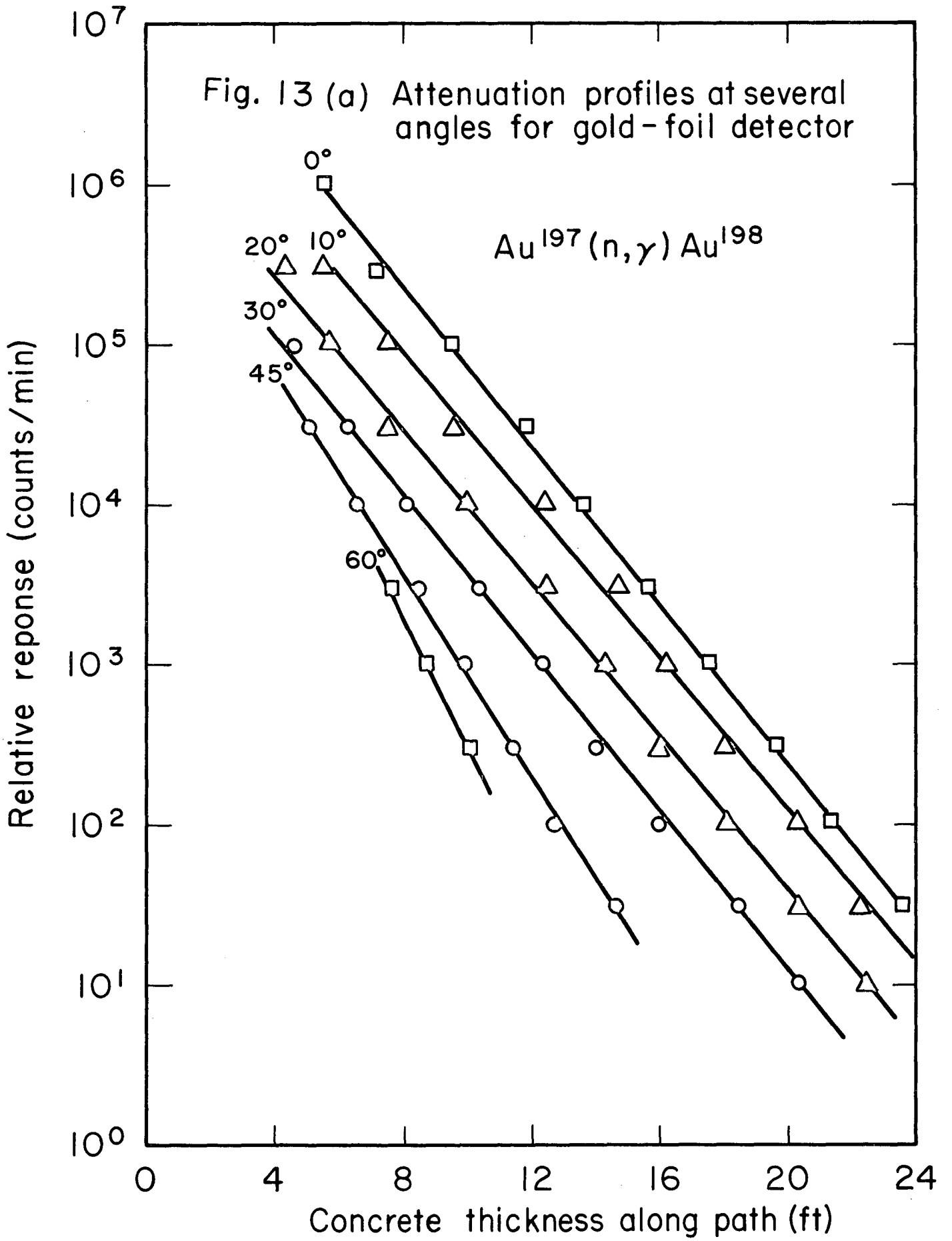
Fig. 13 (a) Attenuation profiles at several angles for gold-foil detector
$Au^{197}(n,\gamma)Au^{198}$
0°
10°
20°
30°
45°
60°
Relative reponse (counts/min)
10^7
10^6
10^5
10^4
10^3
10^2
10^1
10^0
0
4
8
12
16
20
24
Concrete thickness along path (ft)

MUB-4050

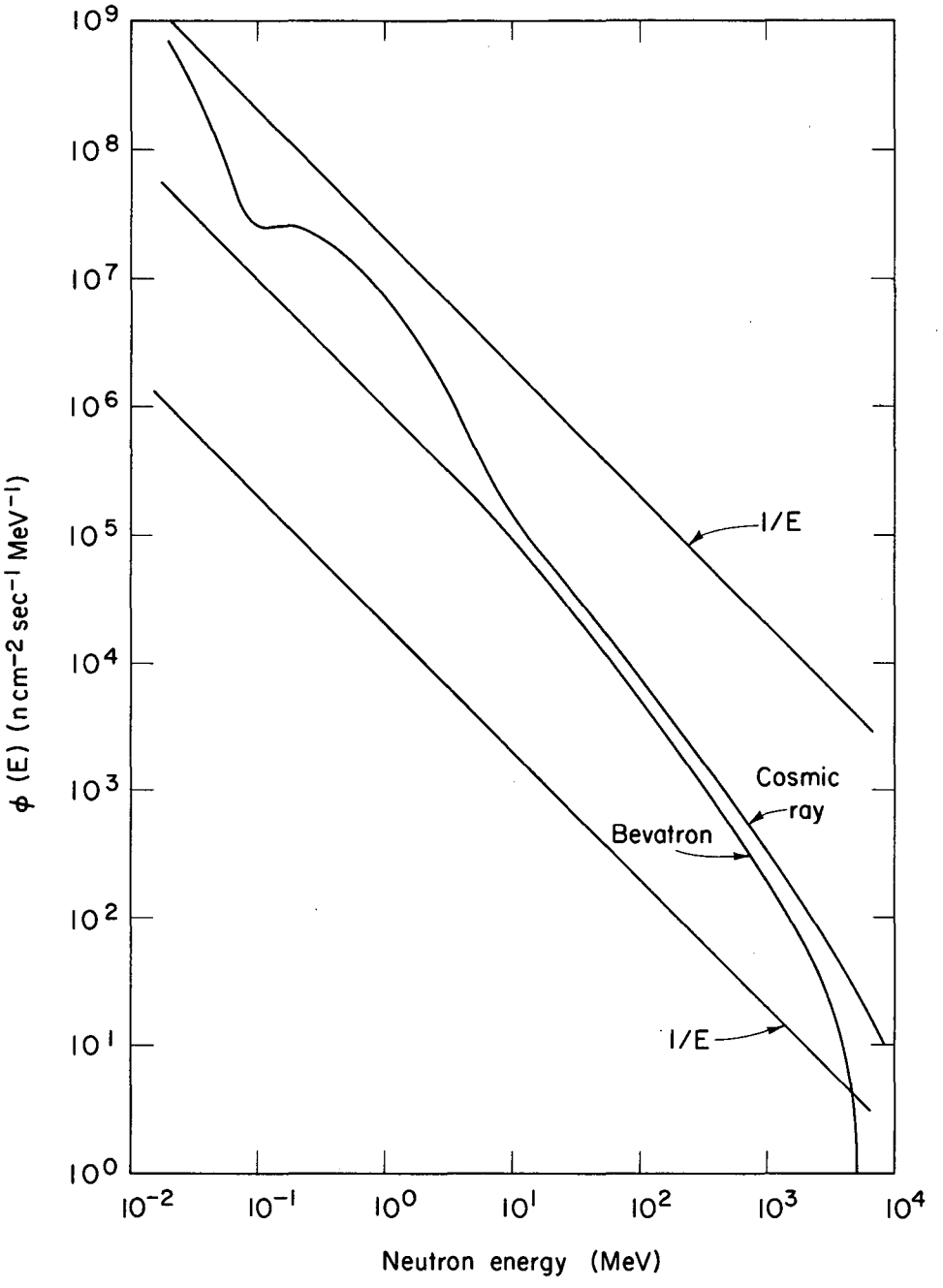
10^9
10^8
10^7
10^6
10^5
10^4
10^3
10^2
10^1
10^0
ϕ (E) (n cm^{-2} sec^{-1} MeV^{-1})
1/E
Cosmic ray
Bevatron
1/E
10^{-2}
10^{-1}
10^0
10^1
10^2
10^3
10^4
Neutron energy (MeV)
MUB-8454

Fig. 18

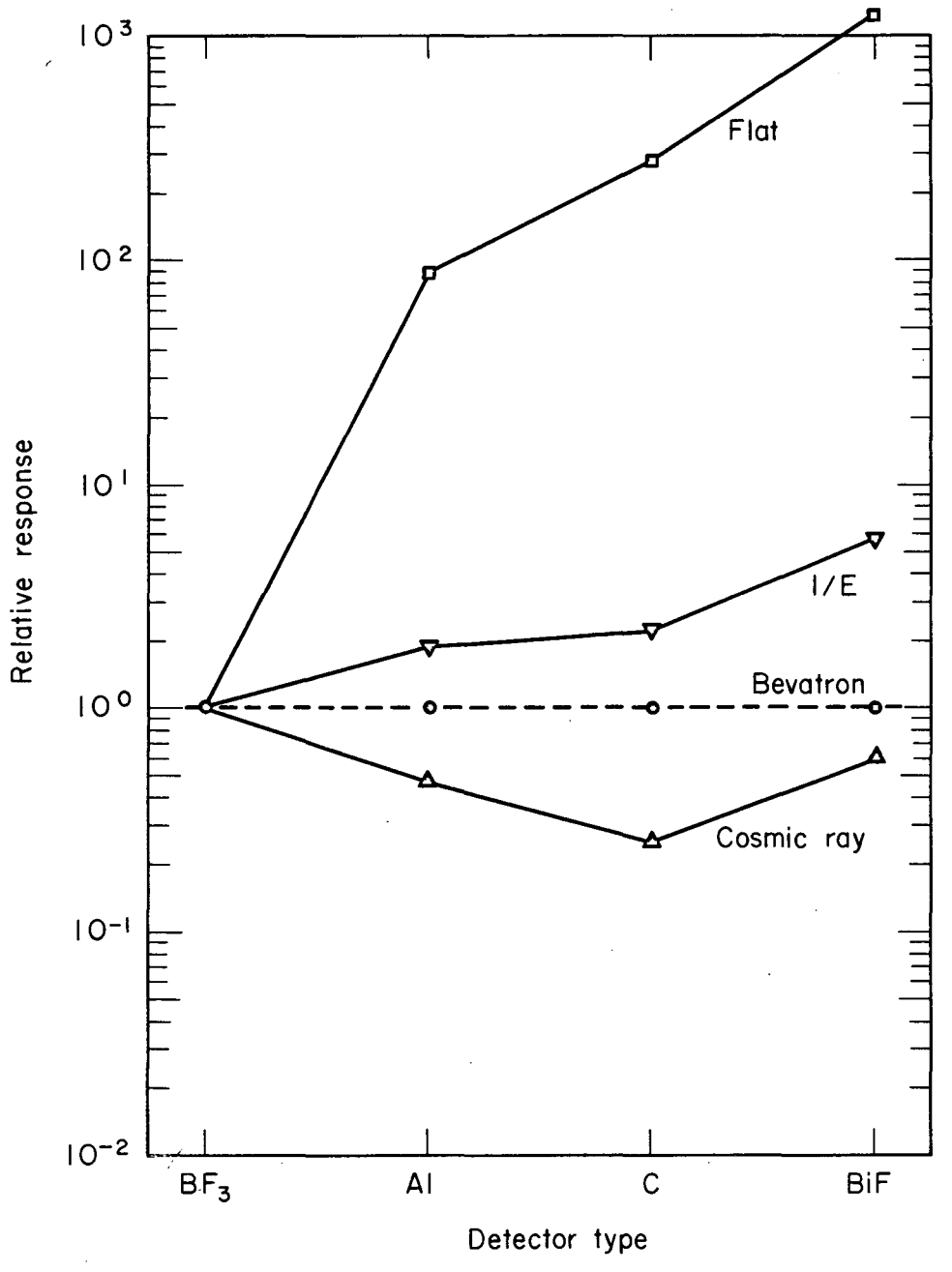

MUB-8455

Fig. 19